

PERIODICA POLYTECHNICA

ELECTRICAL ENGINEERING — ELEKTROTECHNIK

VOL. 4 * No. 2 * 1960



POLYTECHNICAL UNIVERSITY
TECHNISCHE UNIVERSITÄT
BUDAPEST
HUNGARY — UNGARN

PERIODICA POLYTECHNICA

Contributions to international technical sciences published by the Polytechnical University, Budapest (Hungary)

Originalbeiträge zur internationalen technischen Wissenschaft, veröffentlicht von der Technischen Universität, Budapest (Ungarn)

PERIODICA POLYTECHNICA

includes the following series

Engineering
Electrical Engineering
including Applied Physics
Chemical Engineering

The issues of each series appear at quarterly intervals

enthält folgende Serien

Maschinen- und Bauwesen
Elektrotechnik und angewandte Physik
Chemisches Ingenieurwesen

Einzelnummern der genannten Serien erscheinen vierteljährlich

CHAIRMAN OF THE EDITORIAL BOARD — HAUPTSCHRIFTLEITER

Z. CSÜRÖS

EDITORIAL BOARD — SCHRIFTLEITUNG

**N. BÁRÁNY, O. BENEDIKT, S. BORBÉLY, T. ELEK, L. ERDEY, J. GRUBER,
I. KOVÁCS, L. KOZMA, G. SCHAY, K. TETTAMANTI**

EXECUTIVE EDITOR — SCHRIFTLEITER

J. KLÁR

The rate of subscription to a series is \$ 4,00 a year. For subscription or exchange copies please write to

Jahresabonnement pro Serie: \$ 4,00. Bestellungen und Anträge für Tauschverbindungen sind zu richten an:

PERIODICA POLYTECHNICA

BUDAPEST 62, POB 440

ABOUT THE BALANCING OF HALF-WAVE PUSH-PULL MAGNETIC AMPLIFIERS

By

A. FRIGYES

Department of Special Electrical Machines and Automation, Polytechnical
University, Budapest

(Received December 8, 1959)

Nomenclature

A_c	core area of the magnetic material
B_s	flux density at saturation
I_A	current in the output winding of reactor "A"
I_B	current in the output winding of reactor "B"
I_{eff}	r.m.s. value of the maximum allowable current in the output winding of a reactor
I_e	bias current in a circuit balanced with biased rectifier
I_0	output current
N_0	number of turns of the output winding of a reactor
P_0	output power in the basic circuit
P_{sym}	output power in the push-pull circuit
$P_{sym(t)}$	instantaneous value of the output power in the push-pull circuit
$R_A=R_B=R$	ballast resistances
R_c	resistance of the output winding of a reactor
R_0	load resistance
R_i	resistance of the input circuit
U	supply voltage
U_A and U_B	voltage drops across the ballast resistances
U_c	induced voltage in a reactor
U_{cA} and U_{cB}	induced voltages in reactors "A" and "B", respectively
U_0	output voltage
U_i	input voltage

Explanation of indices

av	average value
m	peak value
max	maximum allowable average value in case of some control ranges or circuit arrangements.

Currents and voltages as functions of time are marked with small letters, their average and peak values with capital letters.

On building half-wave magnetic amplifiers of symmetrical output one of the problems arising is how to carry out the balancing of the amplifier elements connected in push-pull in order to keep the response time within 1 cycle, while at the same time obtaining the maximum output for a given core.

In our present investigations the basic circuitry of Ramey will be considered as a basis of comparison. The maximum output of an amplifier built with a given core and winding data in the basic circuit will be determined

Then the ratio of the attainable maximum output to the output of the basic circuitry will be determined when building a symmetrical output circuit from two cores with the same winding data.

In order to elucidate the problem let us start from the basic circuit shown in Fig. 1. Let us suppose that the hysteresis loop of the core is square shaped (Fig. 2.). The characteristic of the basic circuit is shown in Fig. 3 if the input signal is of alternating voltage.

The half-wave magnetic amplifiers are generally used as preamplifiers in control circuits. Their task is to control a further amplifier stage (e. g. magnetic amplifier, rotating amplifier, signal converter etc.). The control of the next stage needs a certain value of current and voltage. It is known, however, that the controllability of the above-mentioned elements is usually determined

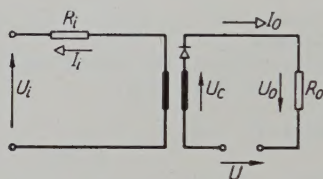


Fig. 1

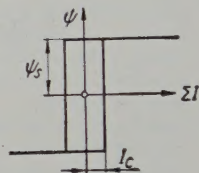


Fig. 2

by the product of some mean value of the current and voltage because e. g. in case of servo-elements to be controlled by the change of the magnetic flux the current and voltage necessary for the control change is in reverse ratio if the number of the exciting turns is changed.

One factor of the valuation of an amplifier is therefore the product of some mean value of current and voltage obtainable from it: the output power. In view of the fact that the effect controlling the next stage generally depends on the linear average value of the output current and voltage, therefore, it is expedient to define the output power as the product of the linear average values of the output current and voltage. The output so defined therefore differs from the power, in the strict physical sense, appearing at the output terminals.

The output of an amplifier changes during control. In this article by the word "output", always the maximum output arising in the course of control, will be meant.

As an amplifier of basic circuit shown in Fig. 1 is completely open in case of $U_i = 0$, the product of the average value of the current flowing through the output resistance and of the average value of the voltage across it, has in this case, to be determined.

The sinusoidal voltage on the core winding cannot be higher than that changing the core flux from the one point of saturation to the other. If the average value of the voltage is denoted U_{cav} then

$$U_{cav} = 4f N_0 A_c B_s \quad (1)$$

The supply voltage to be used cannot be higher than that. In order to secure a good utilisation of the core for the average value U_{av} of the supply voltage

$$U_{av} = U_{cav} \quad (2)$$

to be chosen. Accordingly the supply voltage to be used is determined by the geometric dimensions of the core and the number of turns of the output winding.

The maximum average value of the output current in case of $U_i = 0$ is

$$I_{0av} = \frac{1}{2} \frac{U_{av}}{R_c + R_0} \quad (3)$$

The factor $1/2$ is due to half-wave rectification. From equation (3) the output power is

$$P_0 = U_{cav} \cdot I_{0av} = I_{0av}^2 R_0 = \frac{1}{4} U_{av}^2 \frac{R_0}{(R_c + R_0)^2} \quad (4)$$

P_0 has its maximum possible value if

$$R_c = R_0$$

in which case the current is

$$I_{0av \max} = \frac{1}{4} \frac{U_{av}}{R_c} = \frac{1}{4} \frac{U_{cav}}{R_c} \quad (5)$$

The output power is

$$P_{0 \max} = \frac{1}{16} \frac{U_{av}^2}{R_c} = \frac{1}{16} \frac{U_{cav}^2}{R_c} \quad (6)$$

For the output given by equation (6) only cores of smaller size can be matched. In case of larger cores the current given by equation (5) causes excessive heat in the output windings of the amplifier. In this case the amplifier cannot be matched for the maximum output but the maximum allowable

current should be determined from the heat dissipating capacity of the windings.

The heat caused in the winding depends on the r.m.s. value of the current. Let us denote the r.m.s. value of the maximum allowable current I_{eff} . Since a half-rectified current having a form factor of $\pi/2$ flows through the power windings, thus the corresponding average value is $2/\pi \cdot I_{\text{eff}}$.

If

$$\frac{1}{4} \frac{U_{\text{av}}}{R_c} > \frac{2}{\pi} I_{\text{eff}} \quad (7)$$

then

$$R_0 > R_c$$

is to be chosen so that

$$\frac{1}{2} \frac{U_{\text{av}}}{R_0 + R_c} = \frac{1}{2} \frac{U_{c \text{ av}}}{R_0 + R_c} = \frac{2}{\pi} I_{\text{eff}} \quad (8)$$

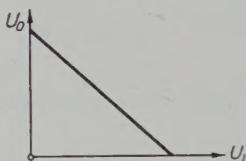


Fig. 3

Hence

$$R_0 = \frac{\pi}{4} \frac{U_{c \text{ av}}}{I_{\text{eff}}} - R_c \quad (9)$$

The output power is

$$P_{0 \text{ max}} = U_{0 \text{ av}} \cdot I_{0 \text{ av}} = I_{0 \text{ av}}^2 R_0 = \frac{U_{c \text{ av}} I_{\text{eff}}}{\pi} - \frac{4}{\pi^2} I_{\text{eff}}^2 R_c \quad (10)$$

It can easily be seen that in the case of limit of the unidentity (7) the equation (10) leads to equation (6).

In the following the output power of the symmetrical circuit will be separately investigated, if the load is matched for the maximum output first (case I) and then for the maximum allowable current in the output winding (case II). The symmetrical circuit is supposed to be built up from cores which in the basic circuit can each be loaded with $P_{0 \text{ max}}$.

In Fig. 4 the three possible methods for balancing are given. In Fig. *a* and *b* the balancing is done by means of passive elements — the resistances R_A and R_B — and by means of the biased rectifiers R_{c3} and R_{c4} , respectively. Fig. *c*

shows a bridge circuit where no passive balancing elements are necessary. It will be shown that from the point of view of maximum output in case I all the three circuits are equivalent, in case II, however, under similar circumstances, from the bridge circuit lower output can be obtained than from the other two circuits.

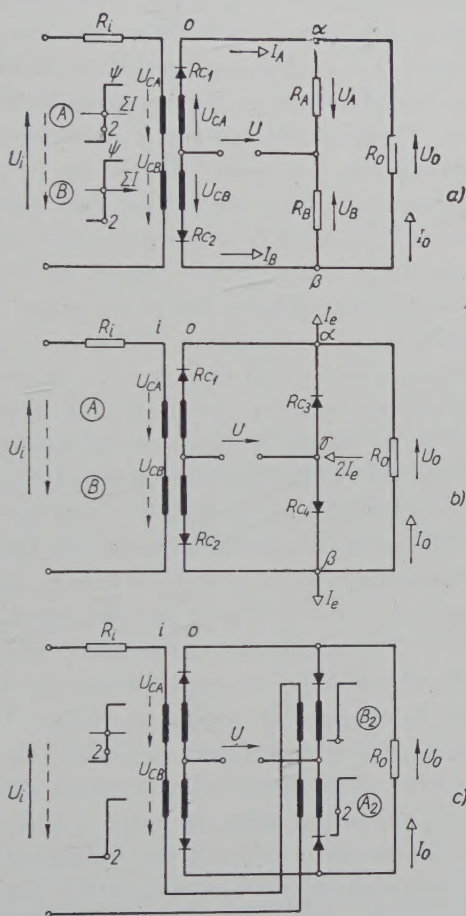


Fig. 4

A) Balancing by means of resistance

The operation method can be followed in Fig. 4a. In the operating half-cycle the direction of the alternating voltage U is marked with the full line arrow. If at the beginning of the operating half-cycle any of the reactors is unsaturated, as a result of the voltage drop on it from U the flux of core „A” gets into the upper, that of core „B” into the lower point of saturation still

in the operating half-cycle (provided, of course, that the voltage U is high enough to deliver the voltage-time integral necessary to saturate the cores. Therefore, it is certain that at the end of the operating half-cycle both cores are in a saturated condition.

In the next half-cycle the rectifiers in the circuit O are blocking. Therefore the change of flux in the cores can be influenced only by U_i . Depending on the direction of U_i in the resetting half-cycle either the flux of core "A", or that of core "B" will be reset. Let us suppose that U_i is an alternating voltage and of such a phase that its direction in the resetting half-cycle corresponds to the dotted line arrow. Theoretically voltage U_i is divided into voltages across the resistance R_i and reactors "A" and "B", on the latter the voltage drops being U_{cA} and U_{cB} whose directions are indicated by the dotted arrow. Therefore the flux of core "A" changes in a downward direction and will thus be reset. The flux of core "B" — however — cannot be changed by the voltage of indicated direction because it is in the lower point of saturation. Consequently voltage cannot appear on reactor "B" ($u_{cB} = 0$) thus the voltage is divided between the resistance R_i and reactor "A". At the end of the resetting half-cycle the flux levels of each core are indicated with the points 2 on the saturation curve in Fig. 4a. In the next operating half-cycle a voltage having a direction marked with the full line arrow would again appear on the reactors. A voltage with such a direction, however, can appear only on reactor "A" and not on reactor "B", on account of the flux of the latter being in the lower point of saturation. Consequently current i_A is zero in a part of the operating half-cycle — until the flux of core "A" gets into the upper point of saturation, — then, after the core "A" has been saturated circuit O of core "A" fires. On the other hand circuit O of core "B" is open during the whole operating half-cycle and the current i_B changes according to voltage U and the resistances of the circuit. As the upper and lower part of circuit O is symmetrical the voltage U_A and U_B have the same instantaneous values after the firing and thus voltage $u_0 = u_B - u_A$ appearing between point α and β is then zero.

The higher is the absolute value of the voltage U_i of a given polarity the higher is the degree to which the flux of core "A" is reset and consequently the higher is the phase angle at which core "A" fires in the operating half-cycle. It can be seen that by increasing the voltage U_i the average of the output voltage increases.

In case of $U_i = 0$ the fluxes of neither core will be reset and thus the output voltage is always zero. Finally when U_i changes its polarity, the flux of core "B" will be reset in the control half-cycle, the flux of core "A" — however — remaining all the time in the upper point of saturation. Thus the average of the output voltage changes its polarity as opposed to the previous case.

The output impedance will be matched to the output terminals α and β . In order to determine the output power let us suppose that during the reset

ting half-cycle preceding the operating half-cycle under investigation the flux of core "A" has been reset as compared to the upper point of saturation, while the flux of core "B" is in the lower point of saturation. As no voltage can appear on reactor "B" the symbol of its winding has been omitted in Fig. 5, and only

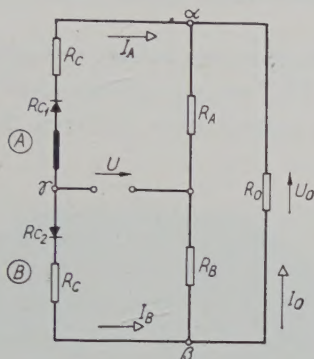


Fig. 5

its resistance R_C is indicated. The forward resistance of the rectifier being incorporated in the resistance of the winding, under these conditions the voltage drop on the rectifier during the operating half-cycle was taken into consideration and it can be omitted in the circuit. Fig. 6 has been drawn

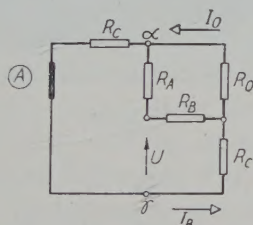


Fig. 6

accordingly. It can easily be seen that Fig. 6 is the same as Fig. 5 excepting the arrangement of the circuit elements. This equivalent circuit applies to a section of the operating half-cycle preceding the firing of core "A". In the circuit, even during this time, flows a current I_B which returns to the terminal marked with the point of the arrow of the voltage source, partly through resistance R_B , partly through resistances R_0 and R_A connected in series. The output current is the component I_0 flowing through output resistance R_0 . This component causes a voltage drop of $I_0 R_A$ across resistance R_A .

On reactor "A" does not therefore appear voltage U as in case of the basic circuit, but a voltage reduced by the drop $I_0 R_A$ across resistance R_A .

Consequently the flux of core "A" changes at a lower rate toward the upper point of saturation and owing to this fact the firing occurs later. The higher current I_0 is or $\int i_0 R_A dt$ voltage-time integral, the later does core "A" fire. The average value of the output current increases with the increase of the firing angle, thus the described phenomenon actually causes an inherent positive feedback.

Fig. 7 shows the voltage across ballast resistances R_A and R_B at an intermediate state of control. The output voltage appearing across the resistance R_0 is proportional to the section lines between the curves.

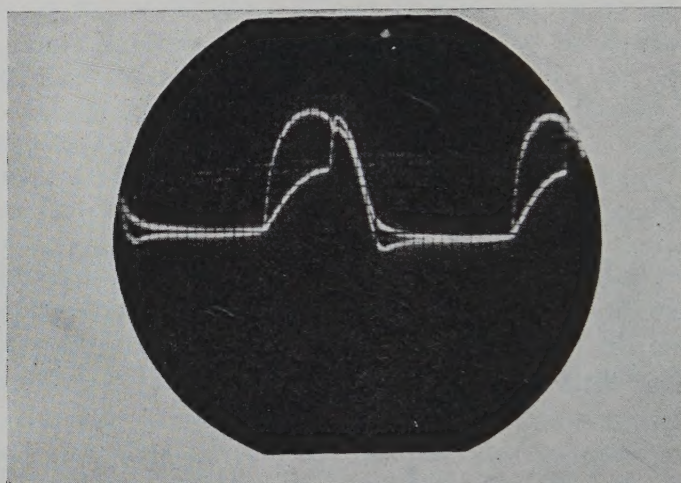


Fig. 7

The operation within 1 cycle is based on the fact that at the end of each operating half-cycle the cores arrive at the border of saturated and unsaturated state independently of the previous state of control. Consequently the "past" of the cores previous to the beginning of the control half-cycle can have no influence on their subsequent "fate".

Let us examine the equivalent circuit in Fig. 6 and let us substitute according to Thevenin's law an equivalent generator for that part of the circuit which is to the right of points $a - \gamma$ (Fig. 8). The voltage U' of this is the voltage appearing on the points $a - \gamma$ of the separated part of the circuit caused by voltage U , and R'_0 is the resultant resistance of the separated circuit to be measured at terminals $a - \gamma$.

$$u' = u - i_0 R_A \quad (11)$$

Based on reasons of symmetry the resistances R_A and R_B must be equal:

$$R_A = R_B = R$$

Taking this into consideration the current i_0 can be expressed as follows:

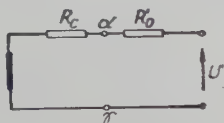


Fig. 8

$$i_0 = u \frac{R}{R_c(2R + R_0) + R^2 + RR_0} \quad (12)$$

Substituting this in equation (11)

$$u' = u \frac{R_c(2R + R_0) + RR_0}{R_c(2R + R_0) + R^2 + RR_0} \quad (13)$$

It can easily be seen from Fig. 8 that prior to the firing the magnetic state of the core and the reaction of the output circuit on the input circuit are described by the same equations as in case of the basic amplifier circuits. The core "A" fires when the $\int u' dt$ voltage-time area equals the reset flux.

If the maximum obtainable output from the symmetrical circuit is to be determined then only that case is to be investigated when core "A" is blocking all through the operating half-cycle. The condition of this of course is that in the preceding resetting half-cycle the flux should be reset with a value of $2 \Psi_s$. The voltage U' is to be chosen so that its half-wave changes the flux of the core with just the value of $2 \Psi_s$. In other words U' must be a sinusoidal voltage for the average of which

$$U'_{av} = U_{cav} \quad (13a)$$

holds.

Considering equation (11) it can be seen that the supply voltage U can exceed U' and thus it can be higher than in the case of a basic amplifier circuit built with the same core and winding data. The voltage increase depends on R_0 and i_0 the latter being dependent on the U itself, besides the other circuit constants. Therefore, it must essentially be determined that in order to attain the maximum output

$$P_{\text{sym max}} = I_{0 \text{ av}}^2 R_0 \quad (14)$$

obtainable in case of a given core at the simultaneous fulfilling of the conditions $U'_{\text{av}} = U_{c \text{ av}}$, which values the freely selectable R_1 , R_0 and U are to have.

According to the results derived in App. I $P_{\text{sym max}}$ has its extreme values both in case of I and II at infinite ballast resistance R and supply voltage U . In case of smaller cores (case I) U and R must approach infinite on the condition that

$$\lim \frac{U_{\text{av}}}{R} = \frac{U_{c \text{ av}}}{4 R_c} \quad (15)$$

where $U_{c \text{ av}}$ is the highest voltage the core is just capable of absorbing [see equation (1)]. At the same time it must be fulfilled that

$$R_0 = 2 R_c \quad (16)$$

as a consequence of which — also according to the equations given in App. I — in case of full control

$$P_{\text{sym max}} = \frac{1}{32} \frac{U_{c \text{ av}}}{R_c} \quad (17)$$

output is obtained on the output resistance. Since at full control core “A” is blocking through the whole duration of the operating half-cycle the current flowing through both ballast resistances is carried by the winding of core “B”. Because for $R \rightarrow \infty$ the other resistances can be neglected while determining the value of the current, therefore the instantaneous value of the current in the winding of reactor “B” is

$$i_B = 2 \lim \frac{u}{R} \quad (18a)$$

The r.m.s. value of this current is

$$I_B = \frac{1}{2} \cdot 2 \lim \frac{U_m}{R} = \lim \frac{U_m}{R} = \frac{\pi}{2} \lim \frac{U_{\text{av}}}{R} \quad (18b)$$

(On account of the half-wave rectification the peak factor is 2 instead of $\sqrt{2}$.) If I_B is higher than I_{eff} corresponding to the maximum allowable temperature rise we have case II (larger cores). In this case

$$\lim \frac{U_{\text{av}}}{R} = \frac{2}{\pi} I_{\text{eff}} \quad (19)$$

must be substituted instead of equation (15) and of course

$$\lim \frac{U_{av}}{R} < \frac{U_{cav}}{4R_c} \quad (20)$$

holds true.

In case II the output has its maximum if

$$R_0 = \frac{\pi}{2} \frac{U_{cav}}{I_{eff}} - 2R_c \quad (21)$$

and its value is

$$P_{sym \max} = \frac{U_{cav} \cdot I_{eff}}{2\pi} - \frac{2}{\pi^2} I_{eff}^2 R_c. \quad (22)$$

It can easily be seen that at the limit when current I_B calculated from equation (18b) equals current I_{ff} allowable for heating considerations case I and II are equivalent.

Namely, if in equations (21) and (22) according to equations (18b) and (15)

$$I_{eff} = \frac{\pi}{2} \lim \frac{U_{av}}{R} = \frac{\pi}{2} \frac{U_{cav}}{4R_c}$$

is substituted for I_{eff} , equations (16) and (17) are obtained. By comparing the equations (6), (7) also (10) and (22) it can be seen that from the push-pull circuit half as much output can be obtained than from the basic circuit built with the same core and winding data. The maximum theoretically obtainable output for $R \rightarrow \infty$ can be well approached if $R = 6-8R_c$ is chosen.

A physical meaning can be attributed to $\lim u/R$ in equation (18a) on the following consideration: The currents caused by voltage u flow through one of the resistances R . In case of $R \rightarrow \infty$ the other resistances in the circuit have no influence on the currents. If either of the cores or both are open the supply voltage appears on the ballast resistances apart from a small differential part. Based on this in the circuit of Fig. 9 for the Y composed of the branches of the supply voltage and the ballast resistances two current generators each supplying a current of

$$i_e = \frac{u}{R}$$

can be substituted. From the afore-said it could be assumed that at point γ of Fig. 5a current $2i_e$ is forced on a circuit, the half of which flows away at point α and the other half at point β . According to this view prior to the firing the upper (a) circuit of Fig. 9 is valid: the current of an instantaneous value of $2i_e$ flowing in at point γ can only flow through the lower core because core

“A” is unsaturated. From this current $2i_e$ the amount of i_e flows away at point β the remaining i_e flowing away through resistance R_0 at point a . The

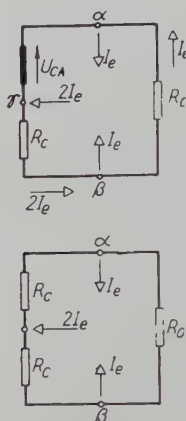


Fig. 9

instantaneous value of the voltage u_{cA} changing the flux of core “A” can be determined by means of the 2nd Kirchhoff’s law applied to the only loop in the figure.

$$u_{cA} = 2i_e R_c + i_e R_0 = i_e (2R_c + R_0) \quad (23)$$

Consequently the blocked core is saturated by the resultant of the voltage drops across the resistances R_c and R_0 due to the current forced through them.

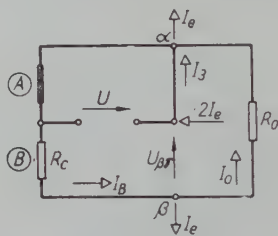


Fig. 10

u_{cA} and $2R_c$ are fixed values in equation (23). From the same equation the current can be determined. It is the current in resistance R_0 being connected to a voltage source of internal voltage u_{cA} and internal resistance $2R_c$. From this latter, however, the maximum output is obtained in case of $R_0 = 2R_c$; i.e. when the internal and external resistances are equal. This corresponds to equation (16).

After the firing the current distribution is according to the lower (b) circuit in Fig. 10. Owing to the perfect symmetry the current in resistance R_0 is zero.

B) Balancing by means of biased rectifiers

According to Fig. 4b, in this circuit rectifiers are used in place of the ballast resistances. The rectifiers are biased from a current generator of infinite internal resistance. The current generator not indicated in the figure supplies the current $2i_e$ in the circuit at point γ . Divided into two equal parts this current flows back at point α and β into the current generator.

The rectifiers are assumed to be ideal; *i. e.* they constitute a short circuit in the forward direction and a break in the reverse direction. Let us suppose that in the resetting half-cycle preceding the operating half-cycle to be investigated the flux of core "A" has been reset, while that of core "B" has remained at the lower point of saturation. Thus at the beginning of the operating half-cycle the reactor "A" is blocking and the reactor "B" is opening. It can easily be seen that the condition of operation is, that prior to the firing a part of the current I_B of reactor "B" is to flow through resistance R_0 until core "A" also fires. Therefore prior to the firing R_{c4} must block otherwise R_0 would be short-circuited by the rectifier and thus no voltage could appear across it. On the other hand R_{c3} must conduct so as to make a closed circuit for the current in R_0 . If the afore-mentioned conditions are given there is a break (between points β and γ) in the branch of rectifier R_{c4} while there is a short-circuit (between point α and γ) in the branch of rectifier R_{c3} . Fig. 10 was drawn accordingly. Core "B" is in saturated condition, therefore, the winding resistance R_c was drawn in its place. Until it fires the negligibly small magnetizing current flows through reactor "A", consequently the circuit of reactor "A" may be assumed to be broken, with the remark, that on account of the conductance of rectifiers R_{c1} and R_{c3} (see Fig. 4b) the total supply voltage appears on reactor "A". Consequently — in opposition to the balancing with ballast resistance — the average of the supply voltage is to be chosen as in case of the basic circuit (see equation 6):

$$U_{av} = U_{cav} \quad (24)$$

A break was assumed in place of the blocking rectifier R_{c4} and the reverse voltage $U_{\beta\gamma}$ was indicated. As all the other rectifiers conduct short-circuits have been put in their place.

As long as the above described conditions exist the circuit is linear and the usual methods for calculating linear circuits can be applied. It is evident that the condition of R_{c3} being conducting and R_{c4} being blocking is the solution of the circuit in Fig. 10 for the instantaneous values

$$u_{\beta\gamma} > 0 \quad (25)$$

and

$$i_3 > 0 \quad (26)$$

presents itself. The following equations can be set up:

$$i_e = i_3 + i_0 \quad (27a)$$

$$i_e = i_B - i_0 \quad (27b)$$

$$u = i_B R_c + i_0 R_0 \quad (27c)$$

As the solutions of the above equations for i_0 , i_B and i_3 the following are obtained:

$$i_0 = \frac{u - i_e R_c}{R_c + R_0} \quad (28a)$$

$$i_B = \frac{u + i_e R_0}{R_c + R_0} \quad (28b)$$

$$i_3 = i_e \frac{2R_c + R_0}{R_c + R_0} - \frac{u}{R_c + R_0} \quad (28c)$$

$$\mu_{\beta\gamma} = u - i_B R_c = u \frac{R_0}{R_0 + R_c} - i_e R_c \frac{R_0}{R_0 + R_c} \quad (28d)$$

Considering equations (25) and (26) the condition of operation is

$$i_e \frac{2R_c + R_0}{R_c + R_0} - \frac{u}{R_c + R_0} > 0 \quad (29)$$

and

$$u \frac{R_0}{R_0 + R_c} - i_e R_c \frac{R_0}{R_0 + R_c} > 0 \quad (30)$$

be fulfilled. Consequently

$$\frac{u}{2R_c + R_0} < i_e < \frac{u}{R_c} \quad (31)$$

By setting the value of the biasing current between these limits the condition of the above described operation can be assured. As the unidentity refers to instantaneous values the value of i_e in the operating half-cycle is to be chosen within the zone marked with lines (see Fig. 11), in such a way, that the output power should be a maximum. Based on equation (28a) the instantaneous value of the output power is

$$P_{\text{sym}(t)} = i_0^2 R_0 = \frac{(u - i_e R_c)^2 R_0}{(R_c + R_0)^2} \quad (32)$$

In case of fixed R_0 the value of $P_{\text{sym}(t)}$ is maximum if i_e has the smallest value given by unidentity (31):

$$i_e = \frac{u}{2R_c + R_0} \quad (32a)$$

This corresponds to the case when rectifier R_{c3} has just been blocking ($i_3 = 0$) but the reverse voltage has not yet appeared on it. Then

$$i_e = i_0$$

and thus

$$P_{\text{sym}(t)} = i_0^2 R_0 = i_c^2 R_0 = u^2 \frac{R_0}{(2R_c + R_0)^2} \quad (33)$$

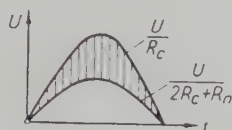


Fig. 11

With varying R_0 the above expression obtains its maximum when

$$R_0 = 2R_c \quad (34)$$

This maximum is

$$P_{\text{sym}(t)\text{max}} = \frac{u^2}{8R_c} \quad (35)$$

(It is to be noted that this circuit also operates with a smaller bias than given by equation (32a). Then rectifier R_{c3} is stressed in the reverse direction and $i_e = i_0$ as the limit of the above discussed. In this case according to equation (32) the output power is decreased as compared to the above given maximum.)

Equation (32a) can only hold true for every instantaneous value if i_e varies sinusoidally in the operating half-cycle; i. e.

$$i_e = I_{em} \sin \omega t$$

where

$$I_{em} = \frac{U_m}{2R_c + R_0} = \frac{U_m}{4R_c} = \frac{\pi}{2} \frac{U_{cav}}{4R_c}$$

In the resetting half-cycle $i_e = 0$ may be true. If it is desired to turn from the instantaneous value of the output power given by the expression (35) to the average value of the same, then keeping in mind that the average of U is

$U_{av}/2$ (this average being effective for the output power) and substituting this for u in equation (35) and also taking (24) into consideration

$$P_{\text{sym max}} = \frac{U_{av}^2}{32R_c} = \frac{U_{c av}^2}{32R_c} \quad (36)$$

This expression is the same as the one (17) derived for the case of balancing with ballast resistances.

C) Bridge circuit

In a bridge circuit amplifier elements are also used in place of ballast resistances and biased rectifiers (see Fig. 4c). The firing of the individual cores is to be controlled in such a way that reactor " A_1 " fire at the same time as reactor " A_2 " and reactor " B_1 " as reactor " B_2 ". Furthermore reactors " A_1 " and " A_2 " are to fire at the upper point of saturation and reactors " B_1 " and " B_2 " at the lower one. In the circuit arrangement of the control windings given in Fig. 4c these conditions are fulfilled, provided the reactors in the opposing branches of the bridge are equal magnetically as well as electrically. Equality can most suitably be ensured by using a common core and winding for the opposing circuit elements.

For the sake of comparison let us assume that cores of the same dimensions and windings with the same number of turns are used as in the circuits given earlier, with the difference, that the output windings are divided into two halves. One half each is used as an output winding of the amplifier elements in the opposing branches of the bridge. Thus the same amount of active material is necessary in the bridge circuit as in the two other circuits. In order to obtain the same utilization of the winding area the same total number of turns and the same wire size are also assumed in the bridge circuit. The resistance of the output winding of a core was denoted earlier R_c . Now the resistance of a half-coil is $R_c/2$. In the basic circuit the highest average value of the sinusoidal voltage that the core can absorb is $U_{c av}$. On account of the half number of turns and the same core dimensions in the bridge circuit a half-coil can absorb the half-wave of a sinusoidal voltage having an average value of $U_{c av}/2$.

As in the earlier cases only the operating half-cycle is now to be investigated. Let us start out from the moment when the flux-level of core " A " has been reset in the preceding resetting half-cycle as compared to the upper point of saturation (point marked 2 in the magnetizing characteristic drawn beside cores " A_1 " and " A_2 " in Fig. 4c) while the flux of core " B " is at the lower point of saturation. The corresponding equivalent circuit is given in Fig. 12. On account of core " B " being saturated no voltages can be induced in coils " B_1 " and " B_2 ", consequently the coils are indicated only by their resistance $R_c/2$. In coils " B_1 " and " B_2 " current starts to flow at the beginning of the

operating half-cycle, and it is sinusoidal all through. This current is output current i_0 flowing in resistance R_0 until core "A" fires. The following voltages are on the half-coils of core "A": Voltage on half-coil " A_1 " between the points δ and α is

$$u_{cA1} = i_0 \frac{R_c}{2} + i_0 R_0 \quad (37a)$$

That on half-coil " A_2 " between the points β and γ is

$$u_{cA2} = i_0 R_0 + i_0 \frac{R_c}{2} \quad (37b)$$

Consequently

$$u_{cA1} = u_{cA2} = u_{cA} \quad (38)$$

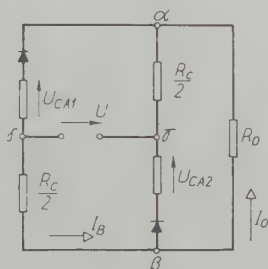


Fig. 12

U_{cA} cannot be higher than that determined by the voltage-time integral of the half-wave which can be absorbed by each half-coil of core "A". In case I the extreme value of the output power is to be sought for in the condition

$$\frac{\omega}{\pi} \int_0^{\pi/\omega} u_{cA} dt = \frac{U_{cav}}{2} \quad (39)$$

According to those derived in App. II the output power has an extreme value if

$$R_0 = R_c/2 \quad (40)$$

and the average value of the supply voltage is

$$U_{av} = \frac{3}{2} U_{cav} \quad (41)$$

Then the extreme value of the output power is

$$P_{\text{sym max}} = \frac{1}{32} \frac{U_{c \text{ av}}^2}{R_c} \quad (42)$$

According to Fig. 12 the instantaneous value of the current flowing in the output winding, prior to the firing of core "A" is

$$i_B = \frac{u}{R_c + R_0} \quad (43a)$$

When matching in accordance with equation (40)

$$i_B = \frac{2}{3} \frac{u}{R_c} \quad (43b)$$

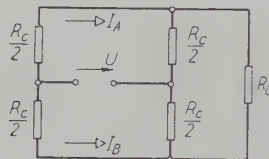


Fig. 13

After firing both cores are open and the corresponding equivalent circuit now valid is shown in Fig. 13. According to this a current of instantaneous value

$$i_A = i_B = \frac{u}{R_c} \quad (44)$$

flows in both branches. This current is 3/2 times as high as that which could be obtained from equation (43b) valid prior to the firing. The heat-dissipating capacity of the amplifier elements is to be checked in the most unfavourable case when the circuit given in Fig. 13 is valid during the whole operating half-cycle; *i. e.* in case of zero control. Then the average value of the current in the output winding of either core is

$$I_{A \text{ av}} = I_{B \text{ av}} = \frac{1}{2} \frac{U_{\text{av}}}{R_c} \quad (45)$$

As earlier, the factor 1/2 is due to the fact that the average of the supply voltage was calculated for the whole cycle (as in case of full-wave rectification)

Although current flows in the output winding only in every other half-cycle. As owing to the half-wave rectification the form factor is $\pi/2$ — according to equation (45) the r.m.s. value of the current in each reactor is

$$I_A = I_B = \frac{\pi}{4} \frac{U_{av}}{R_c}$$

or — taking equation (41) into consideration —

$$I_A = I_B = \frac{3\pi}{8} \frac{U_{cav}}{R_c} \quad (46)$$

It can be seen that the r.m.s. value of the current taken into account from the point of view of heating is now three times as high as in the case of the two other circuits. Consequently the matching for maximum output has to be given up in case of cores smaller than those to be used in the other two circuits. For the same reason the output obtainable from the bridge circuit is reduced, in case of larger cores (case II), when the matching of the output resistance is made for the largest allowable current in the output winding, even in case of the other two circuits.

This drawback of the bridge circuits is reduced by the circuit suggested by LUFKY, SCHMID and BARNHART in which the cores are provided with a third set of windings. The role of these windings is to reset the flux-level of the cores even in the case of zero control, thereby preventing the short-circuiting of the supply voltage through the output windings' own resistances as shown in Fig. 13.

Appendix I

Based on equations (12) and (13) it holds true that

$$i_0 = u' \frac{R}{R_c(2R + R_0) + RR_0} \quad (47)$$

It is expedient to turn to average values.

It must be taken into consideration that the average of the output current determined for the whole cycle is denoted I_{0av} , at the same time keeping in mind, that the instantaneous values of the output current are zero in the second half-cycle. On the other hand, according to equation (13a) U'_{av} means the average of the fully rectified sinusoidal voltage. Therefore, when turning

to average values on the right side of equation (47) the factor $1/2$ is to be written:

$$I_{0\text{ av}} = \frac{1}{2} U'_{\text{av}} \frac{R}{R_c (2R + R_0) + RR_0} \quad (48)$$

By substituting this into equation (14) and taking equation (13a) into consideration, we obtain

$$P_{\text{sym}} = \frac{U_{c\text{ av}}^2}{4} \frac{R^2 R_0}{[R_c (2R + R_0) + RR_0]^2} \quad (49)$$

In this expression $U_{c\text{ av}}$ is a constant given by the dimensions of the core and the number of turns of the output windings according to equation (1). First, let us determine the value of R_0 at which P_{sym} has a maximum, while R is kept constant.

As now $U_{c\text{ av}}$ and R remains unchanged the solution is where the function

$$f(R_0) = \frac{R_0}{[R_c (2R + R_0) + RR_0]^2} \quad (50)$$

has its extreme value. According to the usual method of determining extreme values the solution of equation

$$\frac{\partial f(R_0)}{\partial R_0} = 0$$

is

$$R_0 = \frac{2RR_c}{R + R_c} \quad (51)$$

If the above expression is substituted into equations (49) and (13) for the power

$$P_{\text{sym}} = \frac{U_{c\text{ av}}^2}{32 R_c} \frac{R}{R + R_c} \quad (52)$$

is obtained. The supply voltage is

$$U_{\text{av}} = U_{c\text{ av}} \left[1 + \frac{R}{4 R_c} \right] \quad (53)$$

According to equation (52) P_{sym} increases with the quotient R/R_0 ; i. e. the output power monotonously increases with R and attains its maximum in infinity. The theoretically obtainable maximum of P_{sym} if $R \rightarrow \infty$ is

$$P_{\text{sym max}} = \frac{U_{c \text{ av}}^2}{32 R_c} \quad (54)$$

In case II when the output power is limited by the r.m.s. value of the current in the reactor, the condition of proper matching can be determined in the following way: If the r.m.s. value of the current flowing in the unsaturated reactor is I_{eff} , then owing to the half-wave rectification its average value is $2/\pi I_{\text{eff}}$.

When flowing through the output winding of reactor "B" the current will cause a voltage-drop having an average value of $2/\pi I_{\text{eff}}$ across the resistance R_c . On the other hand, a voltage higher than $U_{c \text{ av}}/2$ must not appear on the unsaturated reactor. On the unsaturated reactor appears in fact the sum of the voltage-drops across resistances R_c and R_0 . Thus the following equation has to be fulfilled:

$$\frac{2}{\pi} I_{\text{eff}} R_c + I_{0 \text{ av}} R_0 = \frac{U_{c \text{ av}}}{2} \quad (55)$$

As the right side of the above equation and the first member of its left side are fixed values, the second member of the right side — this being the output voltage itself — is also determined by the above equation:

$$U_{0 \text{ av}} = I_{0 \text{ av}} R_0 = \frac{U_{c \text{ av}}}{2} - \frac{2}{\pi} I_{\text{eff}} R_c \quad (56)$$

As according to equation (56) the output voltage has a value fixed by the given voltage $U_{c \text{ av}}$ on the reactor and by the current I_{eff} allowed to flow in the output winding, the output power can only be increased by increasing the output current. It can easily be seen that in case of finite R and R_0 values less than a half of the current in reactor "B" will flow through the output resistance. In case of $R \rightarrow \infty$ the average of the output current is just half of the average current $2/\pi I_{\text{eff}}$ flowing in the output winding of reactor "B":

$$I_{0 \text{ av}} = \frac{1}{\pi} I_{\text{eff}} \quad (57)$$

In this case the output power is

$$P_{\text{sym max}} = U_{0 \text{ av}} \cdot I_{0 \text{ av}} = \frac{U_{c \text{ av}} I_{\text{eff}}}{2\pi} - \frac{2}{\pi^2} I_{\text{eff}}^2 R_c \quad (58)$$

The output resistance is to be chosen so that the output voltage-drop U_{0av} caused by current I_{0av} across it, should be as high as determined by equation (56):

$$R_0 = \frac{U_{0av}}{I_{0av}} = \frac{\pi}{2} \frac{U_{cav}}{I_{eff}} - 2 R_c \quad (59)$$

Appendix II

According to the equivalent circuit given in Fig. 12 the instantaneous value of the output current i_0 is

$$i_0 = \frac{u}{R_c + R_0} \quad (60)$$

Correspondingly the instantaneous value of the output power is

$$P_{0(t)} = u^2 \frac{R_0}{(R_c + R_0)^2} \quad (61)$$

But, considering the fact that the extreme value of the above expression is to be determined at a constant voltage $u_c/2$ appearing on a half-coil, let us substitute in the above expression u_c for u according to the following equation:

$$i_0 \left(\frac{R_c}{2} + R_0 \right) = \frac{u}{R_c + R_0} \left(\frac{R_c}{2} + R_0 \right) = \frac{u_c}{2} \quad (62)$$

Hence

$$u \frac{R_c + 2 R_0}{R_c + R_0} = u_c; \quad u = u_c \frac{R_c + R_0}{R_c + 2 R_0} \quad (63)$$

Substituting (63) into (61) we obtain

$$P_{0(t)} = u_c^2 \frac{R_0}{(R_c + 2 R_0)^2}$$

With changing R_0 the above expression has its extreme value in case of

$$R_c = 2 R_0 \quad (64)$$

By substituting this into equation (63) for the supply voltage

$$u = \frac{3}{4} u_c \quad (65)$$

is obtained. Or turning to average values

$$U_{av} = \frac{3}{4} U_{c\ av} \quad (66)$$

Now based on

$$P_{sym\ max} = I_{0\ av}^2 R_0 \quad (67)$$

let us determine the maximum of the output power.

As

$$I_{0\ av} = \frac{1}{2} \frac{U_{av}}{R + R_0} \quad (68)$$

after substituting (64) and (66) we obtain

$$I_{0\ av} = \frac{1}{4} \frac{U_{c\ av}}{R_c}$$

Hence

$$P_{sym\ max} = I_{0\ av}^2 R_0 = \frac{1}{16} \frac{U_{c\ av}^2}{R_c^2} \cdot \frac{R_c}{2} = \frac{1}{32} \frac{U_{c\ av}^2}{R_c} \quad (69)$$

Summary

One of the problems arising in connection with the construction of half-wave push-pull amplifiers concerns the possibility of achieving the maximum possible output of a core of given size. The author investigating the three theoretical possibilities of balancing, shows that in case of properly choosing the circuit constants the circuits are generally equivalent. If the circuit constants are selected according to the method shown in the paper, half of the output is to be achieved in case of any of the three circuits than in that of a basic circuit amplifier built with the same core.

REFERENCES

1. RAMEY: On the Mechanics of Magnetic Amplifier Operation. Trans. AIEE Vol. 70, Pt. II.
2. RAMEY: On the Control of Magnetic Amplifiers. Trans. AIEE Vol. 70, Pt. II.
3. LUFKY-SCHMID-BARNHART: An Improved Magnetic Servo Amplifier, Trans. AIEE Vol. 71, Pt. I.
4. LUFKY-WOODSON: Design Consideration of the Half-Wave Bridge Magnetic Amplifiers, Trans. AIEE Vol. 73, Pt. I.

A. FRIGYES, Budapest, XI., Egry József u. 18., Hungary

PROBLEME DER STOSSFESTIGKEIT VON TRENNSCHALTERN IN MITTELSPANNUNGS-INNENRAUMANLAGEN

Von

A. CSERNÁTONY-HOFFER

Lehrstuhl für Elektroenergie der Technischen Universität, Budapest

(Eingegangen am 20. November 1959)

I.

Die Erfüllung der Anforderungen, die die Koordination der Isolation in Hochspannungsanlagen an die Stoßfestigkeit der Trennschalter stellt, stößt auf zahlreiche Schwierigkeiten. Diese Schwierigkeiten entstammen dem Umstande, daß man aus der dielektrischen Festigkeit, die in einem stark inhomogenen Feld bei einer Spannung von 50 Hz in Erscheinung tritt, kaum auf die dielektrische Festigkeit gegen Stoßwellen mit steiler Stirn zu folgern vermag. Da aber bei einem Trennschalter sowohl zwischen den Polen und der Erde als auch z. B. zwischen den geöffneten Kontakten ein stark inhomogenes Feld besteht, ist es verständlich, daß die Stoßfestigkeit der Trennschalter, deren Isolation vorwiegend für eine Inanspruchnahme von 50 Hz dimensioniert ist, im allgemeinen nicht ausreicht.

Die Anforderungen, die die Koordination an die Stoßfestigkeit der Trennschalter stellt, können kurz wie folgt zusammengefaßt werden:

Die Trennschalter müssen — als Bestandteile der Hochspannungsanlagen — zwischen

- a) den Polen und der Erde
- b) den Phasen und
- c) den offenen Kontakten

eine bestimmte Stoßfestigkeit besitzen.

Da aber ein Durchschlag der Trennstrecken unter allen Umständen vermieden werden muß, müssen die unter a), b) und c) angeführten drei maßgebenden Stoßfestigkeiten *abgestuft* werden, u. zw. in der Weise, daß der für die Stoßfestigkeit der Trennstrecken vorgeschriebene Wert die beiden anderen unbedingt übersteige. (Siehe die kontinuierlich ausgezogenen Linien in Abb. 1.) Diese Forderung wird sowohl in den älteren (1, 2) wie auch in den neueren (4, 5, 6) Regeln und Leitsätzen beachtet.

Infolge der Natur der Koordination stellen jedoch alle drei vorgeschriebenen Werte *untere Grenzwerte* dar, das heißt, *oberhalb* der vorgeschriebenen Minima dürfen die Festigkeitswerte eine beliebige Höhe annehmen, und es

entspringt hieraus nicht die geringste Störung, solange das *Verhältnis* der effektiven Festigkeitswerte nicht kleiner wird als das Verhältnis der vorgeschriebenen Minima. Nach unseren Erfahrungen *verschiebt sich* jedoch mit den effektiven Werten *auch das Verhältnis der effektiven Festigkeiten von dem Verhältnis der vorgeschriebenen Minima in starkem Maße*. Ganz allgemein begegnen wir z. B. dem Fall, daß unter den drei maßgebenden Stoßfestigkeiten *die gegen die Erde den höchsten Wert aufweist*. (Siehe die gestrichelten Niveaulinien der Abb. 1.) Das bedeutet aber, daß die am Trennschalter eintreffende Stoßwelle nicht zur Erde überschlägt, wie es erwünscht wäre, vielmehr schreitet sie — die Trennstrecke überschlagend — fort, oder sie schlägt zu irgendeiner benachbarten Phase über. Die richtige Abstufung kann somit umgestoßen werden.

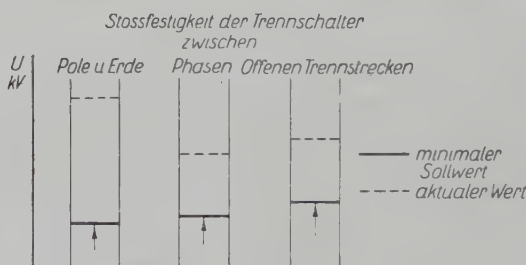


Abb. 1

ungeachtet dessen, daß die Stoßfestigkeit des Trennschalters den erfordernten minimalen Wert in jeder Hinsicht überschreitet, und z. B. den normgerechten IEC-Stoßfestigkeitstest mit Erfolg bestanden hat [4].

Zusammenfassend läßt sich feststellen, daß die richtige Koordination der Trennschalter *durch die Festsetzung der zulässigen minimalen Werte der drei maßgebenden Stoßfestigkeiten allein nicht gesichert werden kann*.

Auf die richtige Koordination können wir uns erst verlassen, wenn die Trennschalter in sich selbst koordiniert sind, das heißt, wenn die Verhältnisse derart beschaffen sind, daß ein Überschlag der Trennstrecken a priori als ausgeschlossen gilt.

Unsere Messungen und Ergebnisse sprechen leider dafür, daß in dieser Hinsicht zahlreiche Typen, ja sogar Konstruktionen der letzten Jahre viel zu wünschen übrig lassen. Aller Wahrscheinlichkeit nach ist dies auf die noch bestehenden Unvollkommenheiten der Regeln und Vorschriften und auf die nicht immer konsequente Ausführung der Stoßprüfungen zurückzuführen.

II.

Zur Klärung der Koordinationseigenschaften von Innenraum-Mittelspannungstrennschalter klassischer Bauart wurden im Hochspannungslabo-

ratorium der Technischen Universität Budapest an mehr als 20 Typen zahlreiche Versuche unternommen.

An den Trennschaltern wurden jeweils alle technisch wichtigen Messungen durchgeführt, an dieser Stelle wollen wir jedoch für jeden Trennschalter lediglich diejenigen Meßergebnisse anführen, die zum Verständnis der zu erörternden Probleme erforderlich sind.

Wir wollen im folgenden die Meßergebnisse von vier Trennschaltern ins Auge fassen. In den Tabellen I und IV wurden die Meßergebnisse an zwei

Tabelle I—IV



50% Überslagspannungen der Trennschalter Nr. I—II—III und IV in kV

Trennschaltern inländischer Erzeugung (10 kV—600 A bzw. 20 kV—600 A) zusammengestellt. Die in den Tabellen II bzw. III angeführten beiden Trennschalter von 10 kV—400 A bzw. 10 kV—200 A sind Erzeugnisse zweier europäischer Weltfirmen.

Am untersten Teil der Tabellen I—IV reihen sich Abbildungen an, die den Charakter der Messungen veranschaulichen. Das Rechteck in der unteren rechten Ecke der Abbildungen deutet das Gestell der Trenner an. Unter den Abbildungen sind die laufenden Nummern der Messungen angeführt. Die 50% Überslag- bzw. Durchschlagspannungen sind durch maßgerechte vertikale Kolonnen veranschaulicht, wobei die Höhe der Spannungen in kV über den Kolonnen angeführt ist. In jeder Kolonne sind auch die von der IEC (3,4)

vorgeschlagenen minimalen Werte durch horizontale Linien angedeutet. (Zu beachten ist, daß sich diese Werte auf nullprozentige Überschlagsspannungen also auf Haltespannungen beziehen.)

Die Kolonnen und Abbildungen in den Tabellen I—IV sind deshalb nicht in der Reihenfolge der laufenden Nummern angeordnet, damit die in der Folge miteinander zu vergleichenden Messungen nebeneinander zu liegen kommen (z. B. Messungen Nr. 3—9, 5—11—16, usw.).

Zur Verbesserung der Übersichtlichkeit sind die Stoßfestigkeitswerte zwischen den Polen und der Erde, U_e , durch graue Kolonnen, die Stoßfestigkeitswerte der Trennstrecken, U_{ts} , durch weiße Kolonnen, die Stoßfestigkeitswerte zwischen den Phasen, U_{ph} , durch schraffierte Kolonnen dargestellt.

Aus den Tabellen geht deutlich hervor, daß zwischen den 50% Überschlagspannungen der Trennschalter und den von der IEC vorgeschriebenen minimalen Stoßhaltespannungen im allgemeinen ein genügend weiter Spielraum besteht. Eine Ausnahme bildet allein der Trennschalter IV, auf den wir später noch weiter eingehen wollen.

Eine um so größere Unzulänglichkeit macht sich demgegenüber bemerkbar hinsichtlich jener Anforderung der Koordination, die sich auf die relativen Größen der drei maßgebenden Stoßfestigkeiten bezieht. Im Interesse der richtigen Koordination sollte nämlich unter den maßgebenden Stoßfestigkeitswerten diejenige zwischen den Polen und der Erde *den geringsten Wert* aufweisen, damit ein Überschlag ausschließlich zur Erde, nicht aber zwischen den Phasen und insbesondere nicht über die Trennstrecken stattfinden könne. Die Meßergebnisse weisen hingegen eben darauf hin, daß im allgemeinen der Stoßfestigkeit zwischen den Polen und der Erde der höchste Wert zukommt: die grauen Kolonnen überragen die weißen und die schraffierten meist ziemlich weit.

Nach Ausweis der Tabellen I—IV liegt die Wurzel dieses Fehlers nicht in einem zu niedrigen Wert der Stoßfestigkeit der Trennstrecken, *liegen doch die U_{ts} Werte überall oberhalb des vorgeschriebenen Minimums*. Die falsche Abstufung verursacht der zu hohe Wert der Stoßfestigkeit zwischen den Polen und der Erde, wobei der Fehler einseitig *nur für den Fall der Stoßwellen negativer Polarität auftritt*.

Wollen wir nun eine richtige Koordination der Trennschalter verwirklichen, ohne an der Konstruktion zu ändern, (was besonders im Hinblick auf die große Zahl der, in den Schaltanlagen eingebauten und falsch koordinierten Trennschalter zweckmäßig erscheint), dann liegt es auf der Hand, daß die allzu hohe Überschlagsfestigkeit der Stützer bei Stoßwellen negativer — und nur bei negativer — Polarität reduziert werden muß.

Um dieses Ziel zu erreichen, wollen wir die Eigentümlichkeiten der Stoßfestigkeit der Stützer näher untersuchen.

Der Umstand, daß die Überschlagsfestigkeit der Stützer polaritätsabhängig ist, stellt eine natürliche Folge der asymmetrischen Form des statischen Feldes dar.

Über den für uns wichtigsten Schnitt des Feldes zwischen den Polen des Trennschalters und der Erde gibt uns die Aufnahme des Feldes im elektrolytischen Trog annähernd Aufschluß. Die Abb. 2 stellt einen solchen Schnitt dar und läßt erkennen, daß das Feld demjenigen zwischen Spitze und Ebene nahe verwandt ist.

Die Phänomenologie der polaritätsabhängigen Festigkeit der Elektrodenanordnung Spitze-Ebene ist allgemein bekannt. Zwar sind die Einzelheiten des Polaritätseffektes physikalisch noch bei weitem nicht geklärt,

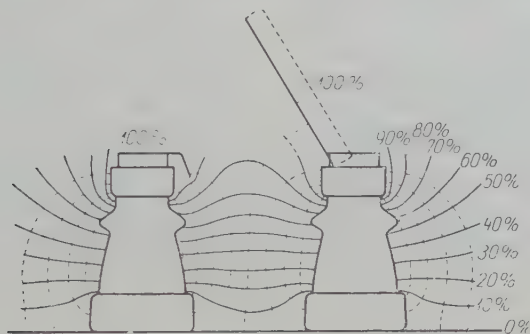


Abb. 2

doch liegt der Grund hierfür möglicherweise darin, daß sich — gleichviel ob die Spitze die negative und die Ebene die positive Elektrode darstellt oder ob das Gegenteil der Fall ist — in der Umgebung der Spitze stets eine positive Raumladung ausbildet. Diese positive Raumladung fördert das Vorwachsen von Streamern im Falle einer positiven Spitze, hindert es dagegen im Falle einer negativen Spitze. Infolgedessen liegt die Durchschlagspannung bei der Anordnung negative Spitze—positive Ebene höher als bei positiver Spitze—negativer Ebene.

Aus diesem Grunde liegt auch die negative Überschlagspannung der Stützer stets höher als die positive, so daß in einigen Fällen (siehe Tabelle III) die negative Überschlagspannung nahezu das Doppelte der positiven beträgt.

Auf Grund der Tatsache, daß die Überschlagspannung in einem asymmetrischen Feld in der Hauptsache von der Form des Feldes um die positive Elektrode abhängt, wollen wir nun folgenden Versuch vornehmen:

Über einer ausgedehnten ebenen Elektrode sei eine andere, kreisförmige Plattenelektrode mit geringerer Fläche so angeordnet, daß die Ebenen der beiden Elektroden einander parallel seien. Ist der Durchmesser der Plattenelektrode z. B. $D = 50$ mm und ihr Abstand von der Ebene $H = 100$ mm, so

wird sich ein stark asymmetrisches statisches Feld ausbilden, wobei die Form des Feldes derjenigen des Feldes zwischen der oberen Kappe eines Stützers und der Erde ähneln wird.

Mißt man die Stoßfestigkeit der skizzierten Anordnung, so erhält man:

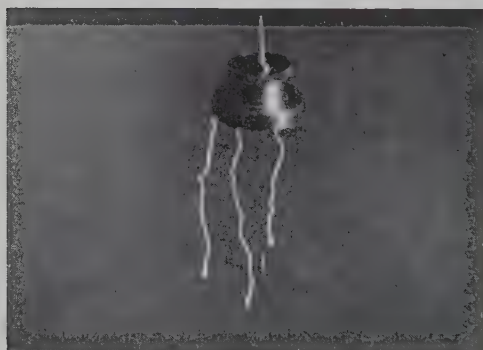
für eine positive Plattenelektrode $U_{+s} = 86 \text{ kV}$,
 für eine negative Plattenelektrode $U_{-s} = 170 \text{ kV}$,



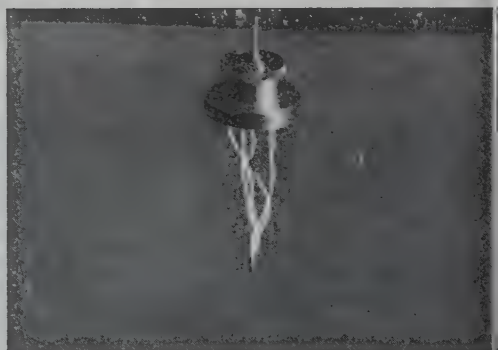
a



b



c



d

Abb. 3

das heißt, die Durchschlagspannung ist wegen der Asymmetrie des Feldes stark polaritätsabhängig.

Die Photographien 3/a und 3/b wurden an Hand dieser Messungen aufgenommen. Aufnahme 3/a zeigt die Durchschläge bei positiver Plattenelektrode und negativer Ebene, während Aufnahme 3/b die Durchschläge bei negativer Plattenelektrode und positiver Ebene darstellt. Aus beiden Abbildungen

geht hervor, daß sich der Durchschlag stets zwischen verschiedenen Punkten der Elektroden ausbildet.

Wir wollen nun an der ausgedehnten Ebene, unter der Plattenelektrode eine $h = 10$ mm hohe Spitze ausbilden und abermals die Durchschlagsspannungen messen. Wir erhalten

für eine positive Plattenelektrode $U_{+s} = 86$ kV

für eine negative Plattenelektrode $U_{-s} = 80$ kV

Es ist auffallend, daß die positive Durchschlagsspannung unverändert bleibt, während die negative um mehr als die Hälfte der ursprünglichen abnimmt. Der Grund für diese Erscheinung erhellt aus den Aufnahmen 3/c und 3/d.

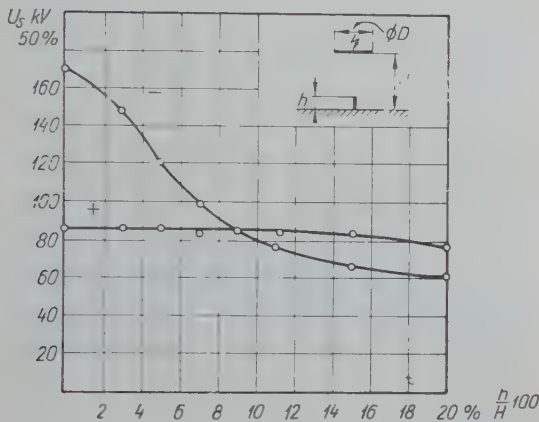


Abb. 4

Die Aufnahme 3/c zeigt die Durchschläge für positive Plattenelektrode und negative Ebene. Aus der Photographie ist deutlich zu erkennen, daß jeder Durchschlag einen anderen Fußpunkt aufweist, und daß die an der Ebene ausgebildete Spitze in dem Durchschlag keine bestimmende Rolle spielt. Es leuchtet somit ein, daß die Größe der Durchschlagsspannung unverändert dieselbe bleibt, wie sie ursprünglich war.

Eine grundlegend andere Lage ergibt sich für den Fall einer negativen Plattenelektrode und positiven Ebene. Gemäß Photographie 3/d befindet sich der untere Fußpunkt der Durchschläge in jedem Fall auf der aus der Ebene herausragenden Spitze. Unter diesen Verhältnissen ist auch die Durchschlagsspannung geringer: An Stelle des im ursprünglichen Zustand gemessenen Wertes von 170 kV beträgt sie nur 80 kV.

In Abb. 4 ist die Durchschlagsspannung in Abhängigkeit von der Höhe h der an der ausgedehnten Ebene ausgebildeten kleinen Spitze dargestellt.

($H = 100$ mm, konstant) Die beiden Kurven, die sich auf positive und negative Stoßwellen beziehen, weisen darauf hin, daß die aus der Ebene herausragende Spitze — bis zu 20% des vollen Elektrodenabstandes „ H “ praktisch allein die Durchschlagspannung — U_s — beeinflusst, wodurch der Ausgleich der ursprünglichen Polaritätsabhängigkeit der Anordnung Spitze—Ebene ermöglicht wird.

Der obige Versuch weist klar auf die einfachste Methode der richtigen Koordination von Trennschaltern hin. Gelingt es nämlich, die negative Überschlagfestigkeit der Stützer auf das Niveau der positiven herabzudrücken, so wird eine am Trennschalter einlaufende Stoßwelle in beliebiger Position des Trenners stets nur zur Erde überschlagen können.

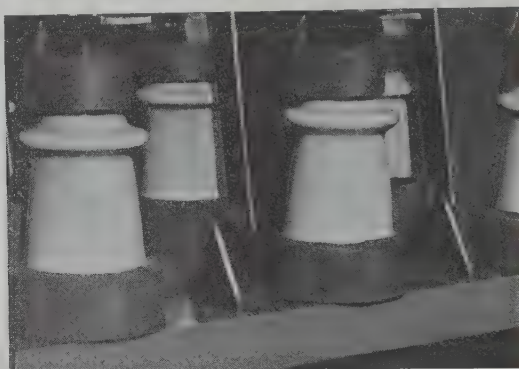


Abb. 5

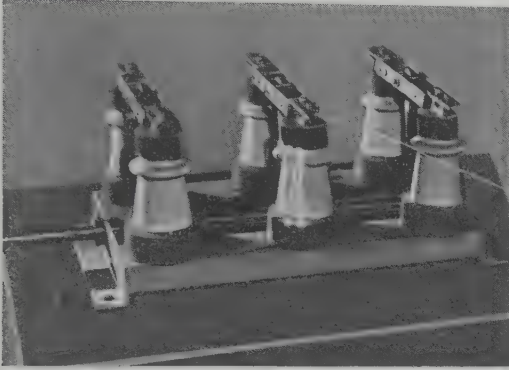
Die praktische Lösung der Aufgabe liegt auf der Hand. Am Gestell — das im asymmetrischen Feld des Trenners der Ebene der Versuchsanordnung entspricht — müssen an geeigneten Stellen irgendwelche Spitzen ausgebildet werden, wobei Größe und Ausbildungsart der Spitzen so beschaffen sein muß, daß sie die 50 Hz Überschlagfestigkeit wenig beeinflusst.

Die aus Abb. 5 ersichtliche Lösung wird diesem Gesichtspunkt in jeder Hinsicht gerecht. An das Gestell werden hiernach in der vertikalen Halbiebungsebene zwischen den Phasen dreieckige Platten angeschweißt. An den 10 kV Trennern I, II und III beträgt die Höhe der Spitzen 60—70 mm, an dem 20 kV Trenner 90 mm.

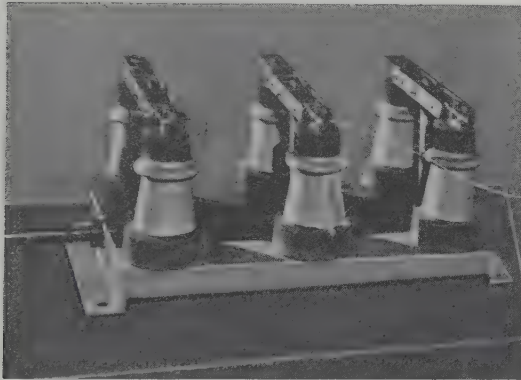
Diese Spitzen reduzieren nun die negative Überschlagspannung der Stützer — ohne die positiv polare zu beeinträchtigen — in dem gewünschten Maße, so daß ein Überschlag an den Trennschaltern ausschließlich zur Erde (zum Gestell) stattfinden kann. In vielen Positionen konnte sogar zwischen den fraglichen Polen ein unmittelbarer Durchschlag überhaupt nicht mehr hervorgerufen werden, was als ideal zu betrachten ist.

Wir wollen nun einige Photographien vorlegen, die im Laufe der Versuche aufgenommen wurden.

Die Aufnahmen 6 a und b betreffen den Trennschalter I, Abb. 6/a zeigt einen Überschlag bei positiver Stoßwelle, die Abb. 6/b hingegen einen solchen bei negativer Stoßwelle, beide im ursprünglichen Zustand des Trennschalters.



a



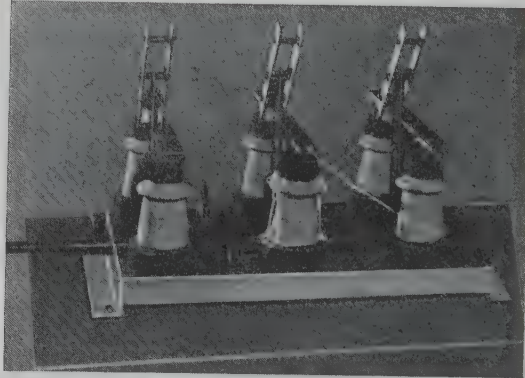
b

Abb. 6

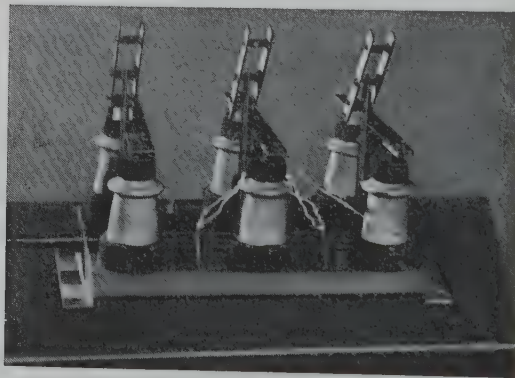
Dieselben Messungen veranschaulichen die Aufnahmen 7/a und 7/b, jedoch an den mit Spitzen versehenen Trennschaltern. Die Aufnahmen lassen deutlich erkennen, daß der Weg der positiven Überschläge unverändert blieb, während die negativen Stoßwellen ausschließlich zu den dreieckigen Spitzen überschlügen.

Es möge schließlich auch die Wirkung der Spitzen auf die 50 Hz Überschlagspannung nicht unerwähnt bleiben.

Bei der 50 Hz Überschlagnspannung der mit hohen Kappen versehenen Trennschalter I, III und IV wurde durch die Spitzen nur eine Herabsetzung von 6%, 4,5% und 0% herbeigeführt, während bei dem auf innengekittete Stützer montierten Trennschalter II — erwartungsgemäß — eine Herabsetzung um 16% beobachtet wurde. (Indessen blieb die Überschlagnspannung noch weit über dem Sollwert.)



a



b

Abb. 7

Was die günstige Wirkung der Spitzen auf die Stoßfestigkeit der Stützer anbelangt, so ist diese Lösung gar nicht als endgültig zu betrachten. Eine beruhigende Lösung kann nur durch die Anwendung neuer, polaritätsunabhängiger Stützen erreicht werden (7, 8). Die beschriebene Methode hat aber den Vorzug, daß die Spitzen auch nachträglich zu beliebiger Zeit montiert werden können, was die richtige Koordination der in den Schaltanlagen eingebauten zahlreichen Trennschalter älterer Bauart ermöglicht.

Die zweite Unzulänglichkeit der Trennschalter besteht — wie schon eingangs in diesem Abschnitt erwähnt — darin, daß ebenso wie Trennschalter Nr. IV auch andere 20 kV Typen die 50% Überschlagspannung der Stützer bei positiver Polarität ungefähr auf dem Niveau aufweisen, auf dem die Haltespannung sein sollte. Dasselbe wurde auch an mehreren 30 kV Typen festgestellt. Zum Glück aber ist nicht nur das Maß dieser Unzulänglichkeit geringer, sondern es kommt ihr auch eine geringere Bedeutung zu, wofür auch der Umstand spricht, daß bei Mittelspannungs-Innenraumtrennern selbst die neubearbeitete VDE 0111/1957 diese Stoßfestigkeitswerte nicht unbedingt als Haltespannungen vorschreibt.

III.

Nachdem in Abschnitt II gezeigt wurde, wie die Mängel der Koordination der Isolation von Trennschaltern durch günstige Beeinflussung des zwischen den Polen und der Erde bestehenden statischen Feldes am einfachsten

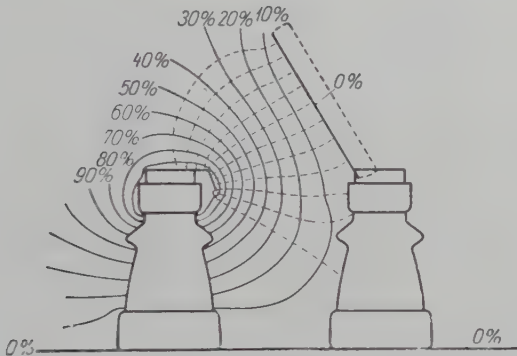


Abb. 8

eliminiert werden können, wollen wir über die Ergebnisse einiger Versuche berichten, die sich auf die Stoßfestigkeit der Trennstrecken beziehen und die bei der Ausbildung neuer Trennschalterttypen nicht außer acht gelassen werden können.


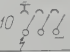
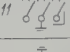
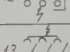
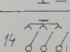

Bei einer Übersicht der Zahlenwerte für die Stoßfestigkeit der Trennstrecken in Tabelle V läßt sich eine starke Polaritätsabhängigkeit feststellen.

Über die Form des zwischen den offenen Kontakten bestehenden statischen Feldes sowie über den Grund der Polaritätsabhängigkeit gibt die im Elektrolyttrog aufgenommene Abb. 8 Aufschluß. Der Abbildung gemäß besteht zwischen den Kontakten ein stark asymmetrisches Feld, dessen Form an das Feld zwischen dem Elektrodenpaar Spitze—Ebene erinnert.

Die Meßergebnisse weisen darauf hin, daß der Polaritätsabhängigkeit der Durchschlagspannung in der Tat der dem Feldbild entsprechende Sinn zukommt, da bei den Messungen mit Stößen *von der Seite der festen Kontakte her* (Nr. 9, 11, 13 in Tab. V) die Durchschlagspannung *negativer* Polarität stets den höheren Wert aufweist: $-U_{ts} > +U_{ts}$.

Werden die Messungen mit Stößen *von der Seite der Kontaktmesser her* vorgenommen, dann wäre auf Grund des Feldbildes eine Umkehrung des Polaritätseffekts zu erwarten, entspricht doch jede der einen Elektrode zugeführte Stoßwelle beliebiger Polarität einer der anderen Elektrode zugeführten

Tabelle V

Mess- anordnung	Durchschlags- spannung	Trennschalter No			
		I 10 kV/600 A	II 10 kV/400 A	III 10 kV/200 A	IV 20 kV/600 A
9 	$+U_{ts}$	105	110	151	155
	$-U_{ts}$	134	177	188	201
10 	$+U_{ts}$	125	143	157	175
	$-U_{ts}$	125	107	156	154
11 	$+U_{ts}$	103	107	150	156
	$-U_{ts}$	134	182	186	198
12 	$+U_{ts}$	121	144	159	178
	$-U_{ts}$	125	107	154	155
13 	$+U_{ts}$	104	107	148	157
	$-U_{ts}$	122	174	171	195
14 	$+U_{ts}$	126	156	158	179
	$-U_{ts}$	116	106	149	152

50% Durchschlagspannung der Trennstrecken in kV

Stoßwelle entgegengesetzter Polarität. Es sollte also bei den Zahlenwerten der Messungen Nr. 10, 12, 14 der Tab. V allgemein $+U_{ts} > -U_{ts}$ gelten.

Dieser Umschlag tritt *bei allen Dreiphasenmessungen* (Nr. 14) und auch bei den Einphasenmessungen Nr. 10, 12, der Trenner II und IV klar hervor.

Bei den *Einphasenmessungen* der Trenner I und III kommt jedoch der Umschlag des Polaritätseffekts nicht zur Geltung, vielmehr findet man statt $+U_{ts} > -U_{ts}$ den Zusammenhang $+U_{ts} \approx -U_{ts}$.

Zu dieser Abweichung muß ausdrücklich bemerkt werden, daß sie in der ganzen umfangreichen Untersuchungsreihe allein bei Einphasenmessungen beobachtet wurde und ausschließlich bei Trennern mit niedrigem Nennstrom und dementsprechend schmalen Messern, eine Tatsache, die auch den Grund der Abweichung anweist.

Der Polaritätseffekt und die Gestaltung der Durchschlagspannungswerte wurde auf Grund des Feldbildes gemäß Abb. 8 erwartet. Bei der Aufnahme des Feldes im Elektrolyt wurde jedoch die Änderung des wahren Feldes in der dritten Dimension vernachlässigt, was zur Folge hat, daß Abb. 8 die wahren

Verhältnisse für einen Dreiphasenstoß der Trennschalter hinreichend, für einen Einphasenstoß jedoch nur in erster Annäherung deckt. Demnach ist es verständlich, daß die Gestalt des Polaritätseffekts *bei Dreiphasenstößen den Erwartungen völlig entspricht*, bei Einphasenstößen jedoch eine Abweichung zu bemerken ist, und zwar eine *um so stärkere, je schmaler die Kontaktmesser sind, und je größer der Abstand zwischen den Phasenleitern bemessen war*.

In obigem wurde die Stoßfestigkeit der Trennstrecke eigentlich qualitativ, vom Gesichtspunkt des Sinnes der Polaritätsabhängigkeit aus betrachtet. Auf Grund des Feldbildes in Abb. 8 sollte sich aber nicht allein der Sinn des Polaritätseffektes umkehren, vielmehr sollten auch *die absoluten Werte der Durchschlagsspannungen* ihre Rolle vertauschen, d. h. die von der einen Seite der Trennschalter her gemessene Durchschlagsspannung positiver Polarität sollte mit der von der anderen Seite her gemessenen Durchschlagsspannung negativer Polarität übereinstimmen und vice versa.

Ein Teil der Meßergebnisse entspricht in der Tat diesen Erwartungen. Ein Vergleich der zusammengehörenden Messungen Nr. 9–10, 11–12, 13–14 der Trennschalter II, III und IV bezeugt nämlich, daß die von der Seite der *festen Kontakte her* gemessenen Durchschlagsspannungswerte *positiver Welle* innerhalb der Streuungsgrenzen mit den von der Seite der *Kontaktmesser her* gemessenen *negativen Werten* übereinstimmen: $+U_{ts9} = -U_{ts10}$, $+U_{ts11} = -U_{ts12}$, und $+U_{ts13} = -U_{ts14}$.

Der Rest der Meßergebnisse folgt jedoch — zum mindesten dem Anschein nach — unseren obigen Erwartungen nicht, da die von der Seite der *festen Kontakte her* gemessenen Durchschlagsspannungswerte *negativer Welle* mit den von der Seite der *Kontaktmesser her* gemessenen Werten *positiver Welle* im allgemeinen nicht übereinstimmen. Es gelten vielmehr die Ungleichungen: $-U_{ts9} > +U_{ts10}$, $-U_{ts11} > +U_{ts12}$ und $-U_{ts13} > +U_{ts14}$.

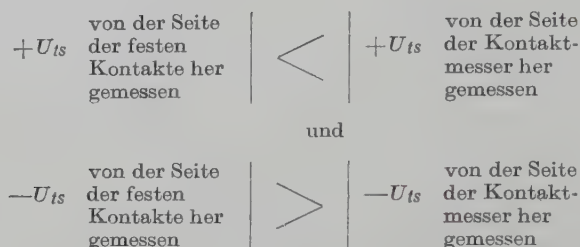
Die zahlenmäßigen Ergebnisse der Messungen deuten somit darauf hin, daß sich in gewissen Fällen Abweichungen von jenen Regelmäßigkeiten ergeben, die auf Grund der Abb. 8 erwartet wurden.

Diese Abweichungen erweisen sich aber — näher untersucht — keinesfalls als »Anomalien«. Die Folgerung nämlich, die wir aus der Form des statischen Feldes der Trennstrecken gezogen haben, kann mit anderen Worten auch so formuliert werden, daß bei einer Stoßprüfung von der Seite der *festen Kontakte her* die negativ polare Durchschlagsspannung höher und die positiv polare niedriger, bei einer Stoßprüfung hingegen von der Seite der *Kontaktmesser her* die positiv polare Durchschlagsspannung höher und die negativ polare niedriger sein muß.

Damit aber dieser Umschlag in den Werten der Durchschlagsspannungen eintreten kann, muß bei der Stoßprüfung, die zuerst von der Seite der *festen Kontakte her* und danach von der Seite der *Kontaktmesser her* durchgeführt wird, der Wert der *negativen* Durchschlagsspannung *abnehmen*, während der

Wert der *positiven* Durchschlagsspannung *zunehmen* muß. In dieser Fassung weisen in der Tat *alle Trennschalter ein einheitliches Verhalten auf*. Zwar sprechen die Zahlenwerte der Tabelle V für sich, doch seien die Meßwerte der Trenner I und IV, die in der Gestaltung des Polaritätseffektes die äußeren Eigenschaften zu verkörpern scheinen, in Tabelle VI separat angeführt.

Die Regelmäßigkeit:



hat sich in der ganzen Versuchsreihe konsequent durchgesetzt, und ist *als allgemeingültig zu betrachten*.

Womit erklärt sich jedoch die Tatsache, daß die *regelrechte Tendenz* nicht in jedem Fall auch zahlenmäßig voll zur Geltung kommt?

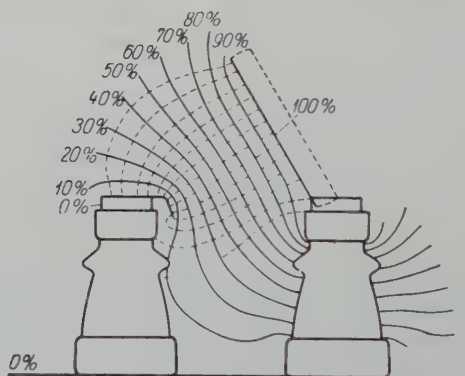


Abb. 9

Als wir im vorigen Abschnitt die Bemerkung machten, daß eine von der einen Seite her einlaufende Stoßwelle beliebiger Polarität einer von der anderen Seite her einlaufenden Stoßwelle entgegengesetzter Polarität entspricht, wurde stillschweigend vorausgesetzt, daß die Form des statischen Feldes bei den von beiden Seiten her vorgenommenen Messungen die nämliche bleibt.

Die Form des statischen Feldes ist jedoch nicht unabhängig davon, ob die Stoßwelle von den festen Kontakten oder von den Kontaktmessern her dem Trennschalter zuläuft. Bezüglich der einem beliebigen Kontakt zulaufenden Stoßwelle befindet sich nämlich die gegenüberliegende Elektrode und die

Umgebung auf dem gleichen (oder nahe dem gleichen) Potential, bei den von den verschiedenen Seiten her vorgenommenen Messungen nimmt somit *bald das Messer, bald der feste Kontakt das Potential der Umgebung an*, wodurch notwendigerweise auch die Form des statischen Feldes beeinflußt wird.

Werden die wichtigsten Schnitte der im Laufe der beiderlei Messungen entstehenden statischen Felder miteinander verglichen (vergleiche Abb. 8 und 9) so wird der Unterschied unmittelbar deutlich.

Tabelle VI


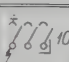

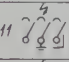
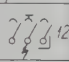
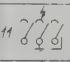
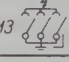

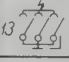
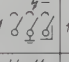
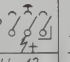
50 % Durchschlagsspannung der Trennstrecken in kV					
Trennschalter No IV			Trennschalter No I.		
9 	+ 155 - 201	▶	175 - 154	10 	9 
11 	+ 156 - 198	▶	178 - 155	12 	11 
13 	+ 157 - 195	▶	179 - 152	14 	13 

Tabelle VII

α°	11 	12 	$+U_{12}$ $-U_{11}$ kV
60	182	144	0,79
45	135	110	0,81
30	88	78	0,88
			im idealen Fall 1,00

50 % Durchschlagsspannung der Trennstrecken in Funktion der Öffnung α°

Es wäre der Mühe wert, auf den Unterschied der beiden Felder näher einzugehen, doch würde dies den Rahmen der vorliegenden Abhandlung überschreiten. Es sei aus diesem Grunde lediglich ein Versuchsergebnis angeführt, das einen anschaulichen Beweis dafür liefert, daß der erwartete Vorzeichenwechsel der Durchschlagsspannungen durch die Störwirkung der Erde beziehungsweise der Umgebung verhindert wird.

Der Einfluß der Umgebung auf das zwischen den offenen Kontakten bestehende statische Feld ist offenbar um so größer, je größer die Trennstrecke ist, und vice versa.

Wenn dies in der Tat so ist, dann kann durch Verringerung des Öffnungswinkels in zunehmendem Maße jener Zustand angenähert werden, in dem die

von der einen Seite her einlaufende Welle beliebiger Polarität der von der anderen Richtung her einlaufenden Welle entgegengesetzter Polarität entspricht. Die Abhängigkeit der Durchschlagspannung von dem Öffnungswinkel α (bei den Meßanordnungen 11–12 des Trennschalters II) ist in der Tabelle VII zusammengestellt.

Aus dieser Tabelle geht klar hervor, daß mit der Verringerung des Öffnungswinkels auch die störende Wirkung der Umgebung vermindert wird, so daß bei einem Öffnungswinkel von 30° der Wert $-U_{ts11}$ dicht an den Wert $-U_{ts12}$ heranrückt.

Die Polaritätsabhängigkeit der Stoßfestigkeit der Trennstrecken darf bei der Konstruktion eines Trennschalters nicht außer acht gelassen werden. Die von einer beliebigen Seite her gemessene Stoßfestigkeit zwischen den Kontakten und der Erde weist nämlich beim negativen Stoß stets einen höheren Wert auf. $-U_s > -U_c$, wogegen für die Stoßfestigkeit über die Trennstrecke die Feststellung gilt, daß, von der Seite der festen Kontakte her gemessen, $-U_{ts} > -U_{ts}$, von der Seite der Kontaktmesser her gemessen, $-U_{ts} < +U_{ts}$ ist.

Hieraus folgt, daß die Trennschalter gegenüber den von der Seite der festen Kontakte her einlaufenden Stoßwellen oft befriedigende Eigenschaften aufweisen, da in diesem Fall die höhere negative und die niedrigere positive Festigkeit zwischen den Kontakten und der Erde mit der ebenfalls höheren negativen und niedrigeren positiven Stoßfestigkeit der Trennstrecke zusammenfällt, so daß letzten Endes ein Überschlag ausschließlich zur Erde stattfinden kann.

Für die von den Kontaktmessern her einlaufenden Stoßwellen gilt hingegen $-U_{ts} < -U_{ts}$, wodurch aber $-$ mit Rücksicht auf den unveränderten Charakter $-U_s > +U_s$ der Stoßfestigkeit der Stützer $-$ ein Durchschlag durch die Trennstrecke bedingt wird.

Bei der Dimensionierung der Trennstrecke ist also folgendes zu beachten: Die ungünstigste Situation entsteht, wenn eine Stoßwelle negativer Polarität von der Seite der Kontaktmesser her dem Trennschalter zuläuft, da die Stoßfestigkeit der Stützer unter solchen Umständen hoch, die Stoßfestigkeit der Trennstrecke aber relativ am niedrigsten liegt. Die Trennstrecke ist also so zu bemessen, daß ihre Stoßfestigkeit auch in diesem Falle unbedingt höher sei als die Stoßfestigkeit der Stützer. Wird dieses Prinzip zur Geltung gebracht, so entspricht $-$ nach unseren zahlreichen Untersuchungen $-$ die Stoßfestigkeit der Trennstrecken unter allen Umständen den Erfordernissen der Koordination.

IV.

Zusammenfassend läßt sich feststellen, daß viele Trennschalter die Koordinationserfordernisse nicht befriedigen, und daß der Grund für die Mängel vornehmlich in der Polaritätsabhängigkeit ihrer Stoßfestigkeit liegt. Da eine

radikale Umformung der Trennschalter vermieden werden soll, muß in erster Linie die Eliminierung bzw. Reduzierung des Polaritätseffektes angestrebt werden.

Es sei an dieser Stelle bemerkt, daß die Methode, die zur Eliminierung der Polaritätsabhängigkeit der Stützer vorgeschlagen wurde, nicht unbekannt ist. Wie aus (9) und (10) hervorgeht, wurde ein solches Verfahren von einigen Firmen bereits angewendet, ohne daß sie allerdings die Grundlagen der Lösung mitgeteilt hätten.

Es sei schließlich der Dank des Autors an Dr. J. Eisler, Professor an der Technischen Universität Budapest, ausgesprochen, der ihm mit seinen wertvollen Ratschlägen stets zur Seite stand.

Auch den Unternehmen, die die Versuchsobjekte dem Autor zur Verfügung stellten sei an dieser Stelle verbindlichst gedankt.

Zusammenfassung

Zur Klärung der Koordinationseigenschaften von Innenraumtrennern klassischer Bauart wurden umfangreiche Versuche unternommen. Es stellte sich heraus, daß die Abstufung der Isolation selbst bei vielen neuen Konstruktionen falsch ist. Der Grund für diese Mängel liegt hauptsächlich in der Polaritätsabhängigkeit der Stoßfestigkeit der verschiedenen Isolationsstrecken.

Die Grundlagen einer Methode, die von einigen Firmen zur Eliminierung des Polaritätseffektes in der Überschlagnspannung der Stützer — ohne weitere Angaben — angewandt wird, werden erörtert.

Der Polaritätseffekt in der Durchschlagspannung der Trennstrecke wird eingehend behandelt, und eine allgemeingültige Regelmäßigkeit festgestellt. Demnach bildet bei Trennern klassischer Bauart stets eine von der Seite der Kontaktmesser her einlaufende negative Stoßwelle den ungünstigsten Fall.

Die Meßergebnisse werden an vier Trennern demonstriert, von denen zwei ungarischer Herkunft, zwei hingegen Erzeugnisse europäischer Weltfirmen sind.

Literatur

1. SEV Publikation 183 (erste Auflage) »Regeln und Leitsätze für die Koordination der Isolationsfestigkeit in Wechselstrom-Hochspannungsanlagen« Bull. SEV 1947 S 869.
2. VDE 0111 Leitsätze für die Bemessung und Prüfung der Isolation elektrischer Anlagen von 1 kV und darüber ETZ 1951 S 671.
3. IEC Publication 71 Recommendations for Insulation Coordination 1954.
4. IEC TC 17/A Proposed Specification for Alternating Current Isolators (Disconnecting Switches) and Earthing Switches 1958.
5. Zweite Auflage der SEV Publikation 183, Bull. SEV 1956 S 941.
6. Neubearbeitung der VDE 0111 1957.
7. SCHERB, E.: Probleme bei Schaltapparaten und Meßwandlern im Zusammenhang mit der Koordination der Isolation Bull. SEV 1957 S 1113.
8. SIROFINSKI, L. I.: Hochspannungstechnik Berlin, Verlag Technik 1955.
9. MATARÉ, H.: Die Koordination der Druckluft-Schnellschalter und Trennschalter BBC Mitteilungen 1943 S 267.
10. ASEA Journal 1957 S 136.

A. CSERNÁTONY-HOFFER, Budapest, XI., Műgyetem rakpart 3, Ungarn.

STATISTICAL QUALITY CONTROL USING AN ANALOGUE COMPUTER*

By

A. AMBRÓZY

Department of Electronic Valves, Polytechnical University, Budapest

(Received October 26, 1959)

1. Introduction

One of the fundamental features of the increasing productivity of the rapidly developing industries is the manufacture of large series. The manufacture of large quantities of a product raise new problems of quality control; for lack of time, instruments and personnel frequently renders it uneconomical for each item to be examined. There may also be a certain time lag between production and control, in which case faults discovered by control cannot, with timely intervention, avoid their repetition.

It was to solve these problems that quality control by sampling was developed on the bases of mathematical statistics. The characteristics of a sample containing the requisite number of items, made to approximate the characteristics of the entire manufactured series with any degree of accuracy desired, while obviating the necessity for an inordinately large number of measurements.

Data obtained from samples, taken during manufacturing, enable production processes to be controlled, for the tendencies of the measured data clearly indicate changes in raw materials, wear of tools etc. The evaluation of the samples is, however, frequently a lengthy process. It is, therefore, worth while to find electric analogies for the statistical relationships and to construct an analogue computer.

2. Statistical relationships [1], [2]

For large series it may be presumed that the characteristic of the product being examined is of normal (Gaussian) distribution. Let the average value of the distribution be m and its standard deviation σ . How can these be determined without measuring the entire series?

* Rewarded by the Hungarian Academy of Sciences.

Let the value of the characteristic measured on the i -th member of a sample containing n items be x_i , in which case the average value is

$$\bar{x} = \frac{1}{n} \sum_{i=1}^n x_i$$

This does not, in general, agree with the average of the large series but very probably falls between the limits

$$m \pm \frac{3\sigma}{\sqrt{n}}.$$

The square of the empirical deviation* of the sample is

$$s^2 = \frac{1}{n} \sum_{i=1}^n (x_i - \bar{x})^2.$$

It is probable that the standard deviation of the sample will be smaller than that of the entire series, since items on the limits of the original distribution only rarely occur in the sample. The probable value of s and σ are therefore related by

$$s = c_n \sigma,$$

where $c_n < 1$ (e. g. for $n = 10$, $c_n = 0.9227$). Evidently s also varies around σ and the extent of this variation as a function of n — also as c_n — is contained in tables. If a sample of many items is used ($n > 15$), then $c_n \rightarrow 1$ and the variation of s is very small.

The average absolute deviation of the members of the sample

$$d = \frac{1}{n} \sum_{i=1}^n |x_i - \bar{x}|$$

and the range

$$R = x_{\max} - x_{\min}$$

are also generally defined.

For normal distributions there are very probable relationships between the expected values of d and R and σ^{**} . It follows, that if the range as well

* The above expression for empirical deviation is used for simplicity of operation, noting that the quantity $\sqrt{\frac{n}{n-1}}$ s , generally defined as "deviation" hardly differs from s , where n is sufficiently large.

** The relationships and tables of the coefficients used in these may be found in the literature [1], [2].

as the average and empirical deviations are found, any departure of the distribution from normalcy can be established.

All four sample characteristics (\bar{x} , s , d , R) may be determined without numerical calculation using an analogue computer and conclusions on the true average and standard deviation may, as has been shown, then be drawn from the samples.

3. Operating principles of the computer [3]

The block diagram of the analogue computer is shown in Fig. 1.

The items ($M_1 \dots M_n$) of the sample are simultaneously placed into the instrument which incorporates n measuring heads. The values ($x_1 \dots x_n$) of the characteristic to be measured are proportionately transformed into alter-

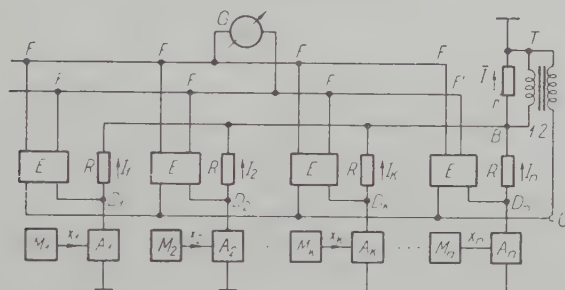


Fig. 1. Block diagram of analogue computer

nating currents $I_1 \dots I_n$ by the transducers A . The currents $I_1 \dots I_n$ flow through a resistance R each and are then connected in junction B . The current through the resistance r is therefore

$$I = \sum_{i=1}^n I_i = C_1 \sum_{i=1}^n x_i,$$

which is related to the average current \bar{I} by $I = n \bar{I}$. An ammeter in series, or a voltmeter across the resistance will therefore, if properly calibrated, give a direct reading of the average value of the characteristic to be measured.

To determine the standard deviation, absolute deviation and range, signals proportional to the differences $I_i - \bar{I}$ have to be produced. The primary windings of a transformer T with a ratio of 1:2 are therefore connected across the resistance r . If the value of r is chosen to be $\frac{R}{n}$ then the average value of the voltage drop on the resistances R due to I_i is the same as that on r due to

$n\bar{I}$. Transforming the latter up by a ratio of 1:2, point C will be equipotential with the point D_k , through which a current of just \bar{I} is flowing. If the current I_i differs from the average, the voltage between C and D_i is proportionate to $I_i - \bar{I}$.

To determine the standard deviation these voltages are applied to rectifiers E with quadratic characteristics, the output current of the i -th of which is

$$I_{Ei} = \beta U_i^2 = \beta R^2 (I_i - \bar{I})^2 = C_2 (x_i - \bar{x})^2,$$

a function of the deviation from the average, where β is a coefficient due to the characteristic of the detector. Connecting the currents from the detectors E in the junctions F and F' the Deprez instrument G will measure the current

$$\sum_{i=1}^n I_{Ei} = \beta R^2 \sum_{i=1}^n (I_i - \bar{I})^2,$$

which is proportional to the variance.

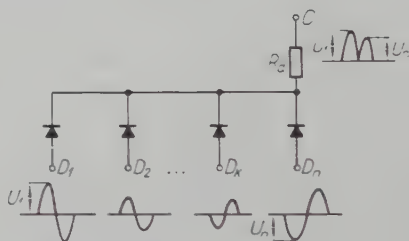


Fig. 2. Range measuring circuit

The measurement of the value of the average absolute deviation is thus straightforward: detectors with linear instead of quadratic characteristics are used, so that the sum of the rectified currents is n times the average absolute deviation.

A simple addition to the circuit of Fig. 1. will also allow the apparatus to be used for measurements of the range. In Fig. 2 (retaining the symbols of Fig. 1) diodes are connected between points $D_1, D_2 \dots D_n$ and point C through a common load resistance R_d . For easy presentation the items to be measured have in the figure been arranged so that the item deviating most in the positive direction is connected to D_1 , while that with the greatest negative deviation is at D_n . The phases of the voltages U_i developing on the various points with respect to C are dependent on the directions of the deviations, for if $I_i > \bar{I}$, the difference voltage is in phase with I_i and *vice versa*. This has also been shown on the figure. Obviously, if R_d is very much greater than the forward resistance of the diode, then in the first half period only the diode

connected to point D_1 will conduct; if it conducts, all the rest will have backward potentials applied to them. Similarly, in the other half-period only the diode of D_n will conduct. The load resistance will therefore develop a signal consisting of half sine curves of different amplitudes. If this signal is connected to a phase-sensitive amplifier the maximum peak-to-peak voltage measured at the output will be proportional to the range.

4. Quadratic detector [4], [5]

It may be seen from the foregoing, that the computer may, for the larger part, be assembled using conventional circuitry, except for the quadratic rectifiers used to measure the variance.

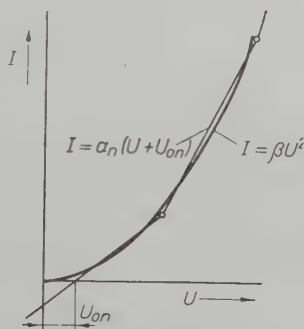


Fig. 3. Approximation to a quadratic parabola

Exact quadratic characteristics are possessed by instruments utilizing the heating or electrodynamic effects of currents. Neither is suited to the present purpose, due to their large power consumption and in the case of the former, the fact that the effect of the temperature of the environment is not negligible. An exact quadratic characteristic may also be obtained by means of an instrument with a bilinear characteristic, based on the Hall effect, but this method is still not feasible. The quadratic portions of the characteristics of electronic valves and semiconductors are too short and not stable.

A quadratic parabola may be approximated at will by a polyangular curve (Fig. 3) produced by means of a network consisting of biased diodes and resistances (Fig. 4). On the initial portion of the curve only diode 1 conducts and the gradient of the curve is determined by the resistance R_1 connected in series with it. At greater voltages diode 2, then diode 3 will begin to conduct, connecting resistances R_2 and R_3 in parallel with R_1 . Since the diodes only function as switching elements, precision and stability depend nearly exclusively on the resistances.

The squaring circuit used in the apparatus should be simple, with few components since — due to the large number of units to be incorporated — their congruence may thus be more easily attained. Fig. 5., being an enlarged part of Fig. 3, will serve to design the network. It is stipulated that the relative deviation of the polyangular curve from the parabola may nowhere be greater than h .

The equation of the parabola is

$$I = \beta U^2,$$

that of the straight line is

$$I' = a_n(U + U_{on}),$$

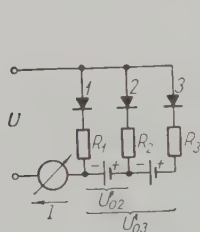


Fig. 4. A circuit to produce a polyangular characteristic

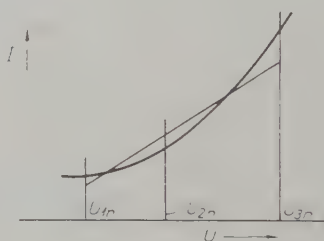


Fig. 5. A straight line section to approximate the parabola

where a_n is the tangent gradient of the n -th straight section and U_{on} is the shift potential of the n -th section. The maximum permitted deviation is

$$I - I' = \pm hI.$$

The ends U_{1n}, U_{3n} of the approximating line (both ends are beneath the parabola) may be found from the equation

$$a_n(U_{1n,3n} + U_{on}) = (1 - h)\beta U_{1n,3n}^2$$

while the position of the point of maximum distance between the chord and the arc, whose abscissa is U_{2n} , may be calculated from the inequality

$$a_n(U_{2n} + U_{on}) - \beta U_{2n}^2 \leq h\beta U_{2n}^2.$$

If a relative deviation of just h is to be permitted at U_{2n} , then the deviation will necessarily be smaller elsewhere and the inequality becomes a mixed second order equation with only one physically real root. This is obviously the coincident pair of roots of the rearranged equation.

Thus

$$(1 + h) \beta U_{2n}^2 - a_n U_{2n} - a_n U_{on} = 0$$

and

$$a_n^2 + 4(1 + h) \beta a_n U_{on} = 0,$$

whence

$$U_{2n} = \frac{a_n}{2\beta(1 + h)}$$

and

$$U_{on} = -\frac{a_n}{4\beta(1 + h)}$$

The positions of the end points are

$$U_{1n,3n} = \frac{a_n \pm \sqrt{a_n^2 + 4(1 - h)\beta a_n U_{on}}}{2\beta(1 - h)}$$

Using the relation obtained for U_{on}

$$U_{1n,3n} = \frac{a_n \pm \sqrt{a_n^2 - \frac{1 - h}{1 + h} a_n^2}}{2(1 - h)\beta}$$

whence

$$U_{1n} = \frac{a_n}{2\beta(1 - h)} \left[1 - \sqrt{\frac{2h}{1 + h}} \right]$$

and

$$U_{3n} = \frac{a_n}{2\beta(1 - h)} \left[1 + \sqrt{\frac{2h}{1 + h}} \right]$$

If $h = 10\%$ is to be permitted,

$$U_{1n} = \frac{a_n}{1.8\beta} 0.576 = 0.32 \frac{a_n}{\beta}$$

$$U_{2n} = \frac{a_n}{2.2\beta} = 0.45 \frac{a_n}{\beta}$$

$$U_{3n} = \frac{a_n}{1.8\beta} 1.424 = 0.79 \frac{a_n}{\beta}$$

$$U_{on} = -\frac{a_n}{4.4\beta} = -0.227 \frac{a_n}{\beta}$$

The ratio U_{3n}/U_{1n} determines the range of a single straight section:

$$\frac{U_{3n}}{U_{1n}} = \frac{U_{3n}}{U_{3(n-1)}} = \frac{0,79}{0,32} \cong 2,5.$$

If, therefore, the abscissae of the breaks are determined by an exponential function of shape 2.5^n , the approximation will be better everywhere by 10%. This would indicate, that a polyangular line with an infinite number of sections is required to approximate a parabola originating at zero. In practice, exploiting the curved characteristic of the first diode, the first break is put between 100—150 mV.

The values of the resistances to be used are plainly

$$\begin{aligned} \frac{1}{R_1} &= a_1 \\ \frac{1}{R_2} &= a_2 - \frac{1}{R_1} \\ &\vdots \\ \frac{1}{R_n} &= a_n - a_{n-1}. \end{aligned}$$

5. Factors influencing precision

The measurement of the average is reduced to a plain measurement of alternating voltage. It is the simplest to use a Deprez instrument with a rectifier for this purpose, which — depending on the class of the instrument — enables precisions of 1—3% to be attained.

An attributive error arises if the alternating voltage to be measured contains harmonics. Harmonics may be generated in the power supply or, more probably, in the possibly non-linear measuring transducers. The second harmonic will probably have the highest amplitude and superimposed on the fundamental harmonic, will once be added to it, next subtracted, thus sharpening one peak and flattening the next of the resultant waveform. A peak rectifying Deprez instrument containing a single diode will then give completely false readings, but if there is a peak-to-peak (two-way) rectification, the effect of the second harmonic may be eliminated. If, however, several harmonics are present it is best to use a selective valve voltmeter tuned to the fundamental harmonic.

The work of the variance meter can be influenced the most by errors in forming averages. If the common resistance r is not exactly an n -th part of R ,

or if the ratio of the transformer is not exactly 1:2, then voltages not exactly corresponding to the average value will be subtracted from the potentials of the measuring points (D_i of Fig. 1). The error thus caused may easily be estimated.

Let the value of the characteristic to be measured again be x_i , the correct average be \bar{x} and the erroneous average be $(1 + \varepsilon) \bar{x}$. The variance computed from the erroneous average is

$$s_h^2 = \frac{1}{n} \sum_{i=1}^n [x_i - (1 + \varepsilon) \bar{x}]^2 = \frac{1}{n} \left\{ \sum_{i=1}^n x_i^2 - \bar{x} \sum_{i=1}^n [2x_i(1 + \varepsilon) - \bar{x}(1 + \varepsilon)^2] \right\}$$

The correct variance is

$$s^2 = \frac{1}{n} \sum_{i=1}^n [x_i - \bar{x}]^2 = \frac{1}{n} \left\{ \sum_{i=1}^n x_i^2 - \bar{x} \sum_{i=1}^n [2x_i - \bar{x}] \right\}$$

The difference between the two is

$$s_h^2 - s^2 = - \frac{\bar{x}}{n} \sum_{i=1}^n \{2x_i \varepsilon - \bar{x} [(1 + \varepsilon)^2 - 1]\}$$

Using the expressions

$$\sum_{i=1}^n x_i = n\bar{x}$$

$$(1 + \varepsilon)^2 - 1 = \varepsilon(2 + \varepsilon)$$

and substituting

$$s_h^2 - s^2 = -2\bar{x}^2 \varepsilon + \bar{x}^2 \varepsilon(2 + \varepsilon) = \bar{x}^2 \varepsilon^2$$

The error is always positive, irrespective of the sign of the error ε , so that the erroneously measured variance is always greater than the correct value. If for instance $\varepsilon = 1\%$ and the relative deviation with respect to the mean value is $s/\bar{x} = 10\%$, the relative error of the relative variance is

$$\frac{s_h^2 - s^2}{\bar{x}^2} : \frac{s^2}{\bar{x}^2} = \frac{s_h^2 - s^2}{s^2} = \frac{\bar{x}^2 \varepsilon^2}{s^2} = 10^{-2},$$

but if $s/\bar{x} = 5\%$ it is $4 \cdot 10^{-2}$. The averaging resistance should therefore be set with special care for samples with narrow distribution patterns.

It has been pointed out, that squaring circuits can by simple methods only be made approximately quadratic. The variance meter is therefore not absolutely precise. The method of design presented secures an error ceiling of 10%. An examination of Fig. 3 shows that the sign of the error changes along the function and it may therefore be expected that if several points of the polyangular curve are simultaneously used for detection then the errors will, to a certain extent, compensate each other. This condition is automatically fulfilled, for the characteristic to be measured differs from the average by different amounts for each item of the sample, so that different difference signals are fed to each of the detectors.

For a more accurate calculation of the error, it is presumed that the difference signals are continuously and normally distributed, with a mean value of zero. The frequency function is then simply

$$f(z) = \frac{1}{\sigma \sqrt{2\pi}} \exp\left(-\frac{z^2}{2\sigma^2}\right)$$

when z is a non-dimensional probability variable proportional to the difference signal (voltage). The variance of this distribution may be obtained if the square of the deviation from the mean be multiplied by the frequency function and integrated between infinite limits:

$$s^2 = \frac{1}{\sigma \sqrt{2\pi}} \int_{-\infty}^{\infty} x^2 \exp\left(-\frac{z^2}{2\sigma^2}\right) dz.$$

Introducing the new variable $w = z/\sigma\sqrt{2}$ and partially integrating:

$$s^2 = \frac{2\sigma^2}{\sqrt{\pi}} \int_{-\infty}^{\infty} w \cdot w e^{-w^2} dw = \frac{2\sigma^2}{\sqrt{\pi}} \left\{ \left[-w \frac{e^{-w^2}}{2} \right]_{-\infty}^{\infty} + \int_{-\infty}^{\infty} \frac{e^{-w^2}}{2} dw \right\} = \sigma^2.$$

as the first term is zero and the second $\sqrt{\pi}/2$. It may be observed that it was necessary to multiply the frequency function by $y = z^2$, the dimensionless form of the ideal detector characteristic.

If a polyangular characteristic is used instead of a parabola, then the mutually relative positions of the breaks and some characteristic point of the distribution have to be determined. Let the polyangular characteristic in our case consist of three sections, and let the upper limit of the uppermost section (-10% deviation; see Fig. 3) be related to point 3σ of the distribution. The

abscissae of the breaks are, according to Chap. 4. (again using the dimensionless variable z)

$$U_{3n} \div z_{33} = 3\sigma$$

$$U_{3(n-1)} \div z_{32} = \frac{3}{2.5} \sigma = 1.2 \sigma$$

$$U_{3(n-2)} \div z_{31} = \frac{3}{6.25} \sigma = 0.48 \sigma.$$

The coefficients a_n are

$$a_3 = \frac{z_{33}}{0.79} = \frac{3\sigma}{0.79} = 3.8 \sigma$$

$$a_2 = \frac{3.8}{2.5} \sigma = 1.52 \sigma$$

$$a_1 = \frac{0.9(0.48)^2 \sigma^2}{0.48} = 0.43 \sigma.$$

In calculating a_3 and a_2 use was made of the expression $\beta = 1$ and a_1 was determined so that the first straight section should connect the origin with a point 10% under the parabola at $z_{31} = 0.48 \sigma$. The approximation to the lower stretch of the parabola is thus worse than was actually the case when making use of the curved characteristic of the diode.

The variance can now be determined in three parts, corresponding to the three straight sections:

$$\begin{aligned} s_1^2 &= \frac{2}{\sigma \sqrt{2\pi}} \int_0^{z_{31}} a_1 z \exp\left(-\frac{z^2}{2\sigma^2}\right) dz = \frac{4\sigma a_1}{\sqrt{2\pi}} \int_0^{w_1} w e^{-w^2} dw = \\ &= \frac{4\sigma a_1}{\sqrt{2\pi}} \left[\frac{e^{-w^2}}{2} \right]_0^{w_1} = \frac{2\sigma a_1}{\sqrt{2\pi}} \left[1 - \exp\left(-\frac{z_{31}^2}{2\sigma^2}\right) \right] \end{aligned}$$

$$\begin{aligned} s_2^2 &= \frac{2}{\sigma \sqrt{2\pi}} \int_{z_{31}}^{z_{32}} [a_2(z - z_{31}) + a_1 z_{31}] \exp\left(-\frac{z^2}{2\sigma^2}\right) dz = \\ &= \frac{2\sigma a_1}{\sqrt{2\pi}} \left[\exp\left(-\frac{z_{31}^2}{2\sigma^2}\right) - \exp\left(-\frac{z_{32}^2}{2\sigma^2}\right) \right] + \\ &\quad + \frac{2(a_1 - a_2)z_{31}}{\sigma \sqrt{2\pi}} \int_{z_{31}}^{z_{32}} \exp\left(-\frac{z^2}{2\sigma^2}\right) dz \end{aligned}$$

$$\begin{aligned}
 s_3^2 &= \frac{2}{\sigma \sqrt{2\pi}} \int_{z_{32}}^{\infty} [a_3(z - z_{32}) + a_1 z_{31} + a_2(z_{32} - z_{31})] \exp\left(-\frac{z^2}{2\sigma^2}\right) dz = \\
 &= \frac{2\sigma a_3}{\sqrt{2\pi}} \exp\left(-\frac{z_{32}^2}{2\sigma^2}\right) + \\
 &+ \frac{2(a_2 - a_3)z_{32} + 2(a_1 - a_2)z_{31}}{\sigma \sqrt{2\pi}} \int_{z_{32}}^{\infty} \exp\left(-\frac{z^2}{2\sigma^2}\right) dz.
 \end{aligned}$$

The integral forming the second term of the results cannot be solved in its closed form, but its value may be found in tables.

Substituting $z_{33} = 3\sigma$ etc. values in these expressions,

$$s^2 = s_1^2 + s_2^2 + s_3^2 = (0.038 + 0.279 + 0.723) \sigma^2 = 1.040 \sigma^2$$

so that the error of the variance is reduced to 4%, which means an error of 2% in the standard deviation.

It is not worth while improving the calculations still further, because the distribution of the sample is — due to the small number of items — only approximately normal. The most significant divergence between the calculated and the actual data is caused by the not continuous distribution of the sample

6. Measurements of the averages and standard deviations of the mutual conductances of electronic valves

The block diagram of Fig. 1 shows that the apparatus may be simply assembled if the transformation of the quantity to be measured does not require a special transducer. Thus, if the grid of an electronic valve has an alternating voltage applied, the alternating current in the anode circuit will be proportional to the control voltage and the mutual conductance. The design of an apparatus to measure average mutual conductances and standard deviations may thus be attempted.

Fig. 6 shows how n electronic valves may, together with the resistances R in their anode circuits, be connected in parallel, with all the anode currents leading through resistance r . The voltage drop on the latter is used, partly to measure the average, and partly, after being boosted by a transformer, to be connected in opposition to the potentials on the anodes. The voltage drops thus obtained are connected to the quadratic detectors, whose outputs are summed.

Anode circuit resistances may not be chosen to be as large as desired. If the resistance r is considered as being composed of n resistances of $n r = R$

magnitude connected in parallel, then obviously there will be $2R$ in the anode circuit of each valve. The alternating voltage in the anode circuit may be calculated from the expression

$$U_a = g_m U_r \frac{2R}{1 + 2R/R_i} = U_r \frac{g_m (2R)}{1 + g_m (2R)/\mu}$$

where U_r is the amplitude of the control voltage at, say, 800 c/s., g_m is the mutual conductance of the valve, R_i is its internal resistance and μ its gain

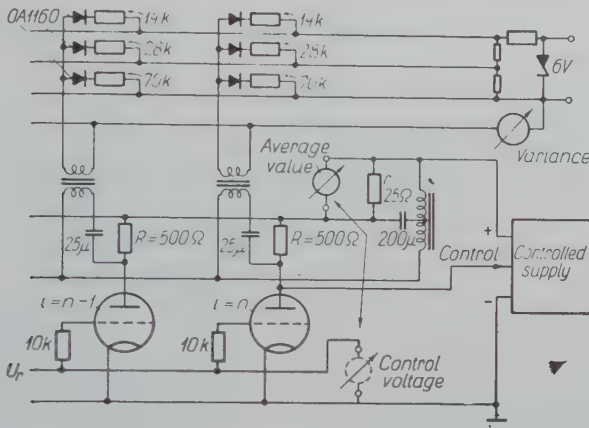


Fig. 6. Circuit diagram of apparatus to examine electronic valves

factor. The second term of the denominator is due to anode reaction, causing a relative error in measurement of

$$\frac{1}{1 + g_m (2R)/\mu} - 1 \approx - \frac{g_m (2R)}{\mu}.$$

In the case of triodes, $\mu = 20 \dots 100$, if 5% inaccuracy is to be permitted, $g_m (2R)$ may be 1 at the most. If it is also considered, that U_r may generally not be more than 1 V, a value of $U_{a \max} \approx 1$ V is obtained. Of this, one half is developed on r , which is sufficient for measurements of the average but not enough to work the quadratic detectors measuring the variance.

The input voltages to the detectors may be increased in two ways. One method is to connect an amplifier before each detector, which might well be transistorized. This is a fairly expensive solution. The voltage drop on the resistance $2R$ may, however, also be increased without undue interference by anode reaction, if we see to it that a minimal alternating voltage is developed on the *anode* with respect to the *cathode*. The circuit shown in Fig. 6 makes provision for this by the proper design of the stabiliser of the power supply.

If the control voltage of the stabilizer is taken straight from the anode terminal (D_n), stabilisation takes place with respect to this point and the supply voltage will not be stable at the point marked $+$, but will incorporate an alternating component just large enough to ensure a minimum alternating voltage on the anode terminal with respect to earth.

The experimental valve measuring apparatus whose circuit is shown in Fig. 6 was constructed at the Department of Electronic Valves of the Technical University of Budapest. The apparatus can accommodate 10 twin triodes

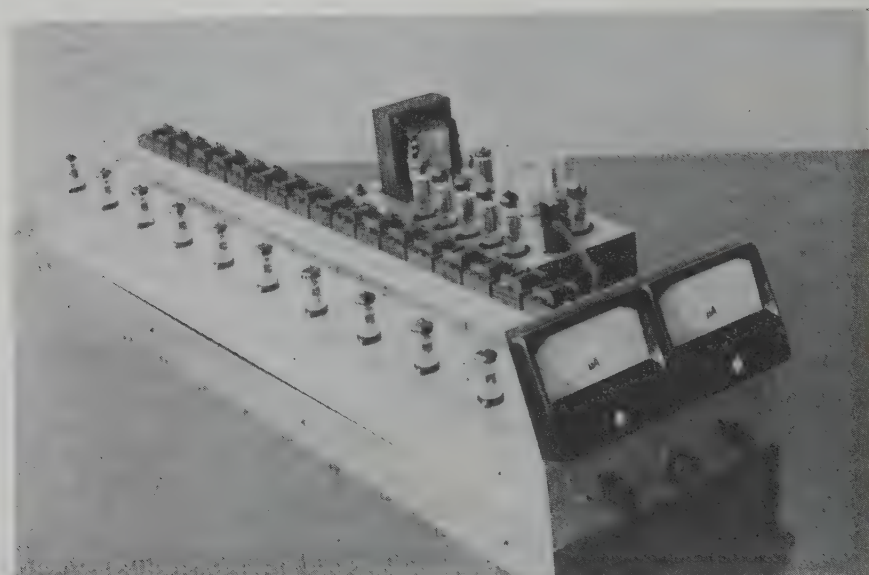


Fig. 7. Photograph of apparatus for examining electronic valves

(ECC 82 or ECC 85) and so computes averages and variances, for a system of $n = 20$ valves. The working point is set by means of the adjustable voltages of the stabilized power supply. The control voltage to the grids is supplied by an external A. F. generator. To ensure precise measurement, the control voltage is measured with the same instrument as that used for the alternating anode voltage. Grid circuit resistances have been included to prevent ultra-frequency swinging and anode circuit transformers and capacitors to achieve D. C. separation of the variance meter network. The diodes of the quadratic detectors were biased by voltages stabilized with a Zener-diode. A photograph of the apparatus may be seen in Fig. 7. The unit on the left of the photo accommodates the valves to be measured. To their right, are the anode circuit transformers. The instrument panel mounts the average indicator Deprez instrument on the left, the variance meter on the right. The special stabiliser that was described is on the right hand side of the photo.

10 ECC 82 and 10 ECC 85 type valves were examined with the apparatus. Column 1 of Table I contains the symbols for the 20 systems of the 10 ECC 85 twin triodes. Column 2 has the individually measured mutual conductances of the valves (each the mean of 2 readings), and column 3 shows the deviations from the average. Column 4 contains the difference voltages measured between points C and D_i of the apparatus (Fig. 1) in mV (each the mean of 8 readings). A 1% difference in mutual conductance ($= 0,066 \text{ mA/V}$) here corresponds to 26 mV. The calculated average and the relative deviation calculated from the data of columns 3 and 4 are shown at the bottom of the table. The instruments in the apparatus then showed $\bar{g}_m = 6,45 \text{ mA/V}$ and $\frac{s}{\bar{g}_m} = 10,4 \%$, which is a very good approximation to the calculated values. All readings were taken at the working point stated in the catalogue.

Table I

	$g_m \text{ (mA/V)}$	$\Delta g_m \text{ (mA/V)}$	$\Delta U \text{ (mV)}$
1/a	6.45	-0.15	- 30
b	6.95	+0.35	+110
2/a	8.45	+1.85	+620
b	6.1	-0.5	-430
3/a	6.85	+0.25	+ 60
b	6.6	0	0
4/a	7.4	+0.8	+240
b	7.0	+0.4	+150
5/a	6.35	-0.25	-120
b	7.15	+0.55	+230
6/a	5.4	-1.2	-530
b	6.35	-0.25	-100
7/a	6.05	-0.55	-180
b	5.6	-1.0	-430
8/a	7.2	+0.6	+270
b	7.45	+0.85	+350
9/a	5.75	-0.85	-370
b	6.5	-0.1	- 50
10/a	6.3	-0.3	-150
b	6.6	0	+ 50

$$\bar{g}_m = 6,6 \text{ mA/V} \quad s_{gm} = 0,698 \text{ mA/V} \quad s_{\Delta U} = 283 \text{ mV}$$

$$\frac{s_{gm}}{\bar{g}_m} = 10,6 \% \quad \frac{s_{\Delta U}}{\bar{U}} = \frac{283}{2600} = 10,9 \%$$

The sum of the figures of column 4 is not zero, but -310 mV. This means that the averaging resistance was not properly set, because $-310:20 = -15.5$ mV were added to the voltages of each of the measuring points, corresponding to an error of over 0.5% in setting. In the case considered, this did not noticeably influence the variance value obtained.

Similar measurements were also carried out with type ECC 82 valves, where the following is a brief summary of the results obtained:

Average mutual conductance according to individual

measurements	1.92 mA/V
Indicated mutual conductance	1.85 mA/V
Calculated variance according to individual measure-	
ments	11.6%
Calculated variance according to voltage differences .	14.1%
Indicated variance	13.1%

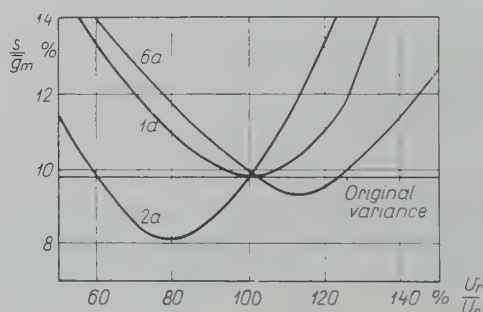


Fig. 8. Change of variance for changes of the mutual conductance of one valve

It was noted that the mutual conductance of one of the valves considerably varied with time, which explains the differences of the variance values that were measured at different times. The mutual conductance of this same valve was, incidentally, some -50% different from the mean, thus considerably increasing the calculated variance, while not increasing the measured variance to a similar extent, as the valve was well outside the normal functioning range of the quadratic detector. After changing this valve, the variance decreased to below 9% .

To control the variance meter the following experiment was carried out: The grid of one of the triodes was disconnected from the rest and a control voltage of variable amplitude, coherent with the common control signal was applied to it. Changes in the control voltage changed the apparent mutual

conductances of the valve, thus altering the average mutual conductance and especially the variance. The readings are shown in Fig. 8.

Valve 1a is of nearly average mutual conductance. Correspondingly, at 100% control voltage the variance reading does not change with respect to its original value, but a decrease or increase in control voltage increases the variance. The mutual conductance of valve 2a is a great deal over the average. If about 80% control voltage is applied its apparent mutual conductance attains the average and the variance considerably decreases. A similar result can also be attained with valve 6a if the control voltage is increased to 115%.

Interesting results are shown in Table II. The average and the variance of mutual conductivity were measured for different values of heater voltage. It was found that while variance for normal heater voltage was acceptable, it decreased somewhat during overheating and increased considerably by underheating.

Table II

U_f (V)	\bar{g}_m (mA/V)	s/\bar{g}_m %
5.0	3.85	20.5
5.5	5.8	12.5
6.3	6.55	10.4
7.0	7.1	9.0

7. Applications

Apparatus for measuring averages, variances and ranges cannot only be used for measuring the mutual conductances of electronic valves. The direct current through electronic valves at the working point may, for instance, also be controlled after having, of course, first been converted to alternating current. The simplest way of doing this is periodically to cut the valve off.

A 1:1 ratio square wave voltage is connected to the grid, whose positive peak value is the bias corresponding to the working point to be measured (this may be kept at a constant value with a fixing diode), while the negative peak completely cuts the valves off. The current through the common anode load will then have a peak-to-peak amplitude of

$$nI_0 = \sum_{i=1}^n I_{0i}$$

where I_{0i} is the working point current of the individual valve. The average measuring instrument is calibrated in working point current, with due attention to the wave-shape factor of the square wave signal.

The measurement of variances can also take place by the method described for sine waves, but care must be taken to secure adequate impulse transfer through the transformers.

The apparatus described in Chap. 3 and shown on Fig. 1 may be used without transducers in all cases where the quantity to be measured is a current, or proportional to a current, *e. g.*

$$G = \frac{I}{U}$$

in the case of a conductance. Measurements may thus be made of the output conductances, mutual conductances and even the current amplification of transistors. Similarly the current

$$I = U j \omega C$$

through a condenser is proportional to the capacity and the apparatus is thus suited for the control of mass produced condensers.

In measuring resistances or parameters resembling resistances allowance has to be made for certain errors. Let n resistances of values $R_1, R_2 \dots R_n$ be connected in parallel. The apparatus will measure the parallel resultant proportional to the total current flow

$$\frac{1}{R_e} = \frac{1}{R_1} + \frac{1}{R_2} + \dots + \frac{1}{R_n}$$

Writing the components as $R_i = \bar{R} + \Delta R_i$

$$\frac{1}{R_e} = \frac{1}{\bar{R} + \Delta R_1} + \frac{1}{\bar{R} + \Delta R_2} + \dots + \frac{1}{\bar{R} + \Delta R_n} = \frac{1}{\bar{R}} \sum_{i=1}^n \frac{1}{1 + \Delta R_i / \bar{R}}$$

which may be developed into a binomial series according to the second term of the denominator, *i. e.* the relative difference. Terminating the series with the second term we obtain

$$\begin{aligned} \frac{1}{R_e} = \frac{1}{\bar{R}} \left[n - \left(\frac{\Delta R_1}{\bar{R}} + \frac{\Delta R_2}{\bar{R}} + \dots + \frac{\Delta R_n}{\bar{R}} \right) + \left(\frac{\Delta R_1}{\bar{R}} \right)^2 + \right. \\ \left. + \left(\frac{\Delta R_2}{\bar{R}} \right)^2 + \dots + \left(\frac{\Delta R_n}{\bar{R}} \right)^2 \right] \end{aligned}$$

The definition of the mean tells us that

$$\sum_{i=1}^n \frac{\Delta R_i}{\bar{R}} = 0$$

and using

$$V^2 = \frac{1}{n} \sum_{i=1}^n \left(\frac{\Delta R_i}{\bar{R}} \right)^2 = \frac{1}{\bar{R}^2} s^2$$

(V being the variation coefficient or relative variance) whence, eliminating the quadratic terms

$$\frac{1}{R_e} = \frac{n}{\bar{R}} + \frac{1}{\bar{R}} nV^2$$

The current through the measuring resistance is proportional to $\frac{1}{R_e}$ and the average value thus obtained is

$$\bar{R}' = nR_e = \bar{R} \frac{1}{1+V^2}$$

which is less than it should be. If, for instance, $\pm 20\%$ resistances are being examined which all fall within the given tolerance limits then, presuming normal distribution, the value of V is obtained from the condition

$$\pm \frac{3s}{\bar{R}} = \pm 3V = \pm 20\%$$

as it is very probable that all resistance values will be within three times the variance limits in the positive and negative directions. Then $V = 6.7\%$ and

$$\bar{R}' = \bar{R} \frac{1}{1 + 45 \cdot 10^{-4}} \approx \bar{R}.$$

The difference is insignificant. It may similarly be proved that though conductances are measured instead of resistances, the variance of resistances is obtained with small errors.

In conclusion, it should be pointed out, that the computer described in this paper is primarily suited to the evaluation of electric parameters or in cases where simple transducers can be used.

The possibility of using a pneumatic analogue of this apparatus to measure lengths in engineering should be investigated, making use of the analogies between differences of pressure and voltage and of volume velocity and current.

Acknowledgement

I should like to thank I. P. Valkó, Director of the Department (who made it possible for the experimental apparatus to be built within the research program of the Department) for the valuable advice given in the preparation of this paper.

Summary

Quality control in modern mass production is usually made by sampling. The statistical evaluation of the measurements, however, frequently requires much time. The Department of Electronic Valves of the Technical University of Budapest is, therefore, developing a computer which by means of electric analogies instantaneously determines the average value, variance, range or any other statistical property of the characteristic to be controlled, from a sample consisting of numerous items. Transducers convert the values of the characteristics to proportionate alternating currents. The apparatus sums the currents to present the average value and by squaring the differences between the average and the individual values and summing the squares presents the variance, both by direct reading. The model that was built is for controlling the mutual conductances of electronic valves.

Literature

1. Statisztikai minőségellenőrzés. Szerkesztette Vincze István (Statistical Quality Control. Edited by I. Vincze). Közgazdasági és Jogi Könyvkiadó, Budapest 1958.
2. SCHAAFSMA, A. H., WILLEMSE, F. G.: Moderne Qualitätskontrolle. Philips Technische Bibliothek, 1955.
3. Hungarian patent registered. N° Ao-216.
4. BURT, E. G. C., LANGE, J. H.: Function generators based on linear interpolation with applications to analogue computing. Proc. I. E. E. **102**, 856 (1955).
5. WAHRMANN, C. G.: A true RMS instrument. Brüel — Kjaer Technical Review 1958. N° 3, p : 9.

A. AMBRÓZY, Budapest, XI., Stoczek u. 2., Hungary

THEORETICAL METHODS CONCERNED WITH THE ASYNCHRONOUS OPERATION OF TURBO-GENERATORS

By

F. CSÁKI

Department for Special Electric Machines and Automation,
Polytechnical University, Budapest

(Received February 17, 1960)

Introduction

Reviewing the fundamental books discussing the transient phenomena and behaviour of the synchronous machines [2, 3, 14, 23, 16, 18, 22] it may be stated that for most of the transient phenomena a clear explanation could be found. Examining, however, the material elaborated, it becomes conspicuous that the theoretical results refer mostly to machines operating with a constant angular speed, or speed of rotation. Even if there is an obvious change (*e. g.* at asynchronous strating, or synchronizing), the angular speed is frequently assumed to be constant at least at a certain initial period, as this simplifies the discussion of the problem.

A variable speed leads namely to a nonlinear differential equation system. The difficulties in solving nonlinear differential equations are explanations for the fact the cases of the synchronous machines with variable speeds having not been dealt with in details, but lately [15, 33, 36, etc.], though raising the problem may look back upon a past of many decades [*e. g.* 13, 32] and almost in every transient phenomenon there must be a change in the speed. To avoid the nonlinear differential equations, when discussing the cases with variable speeds, the starting point is many times the prescribed motion of the rotor, *e. g.* a change of small amplitude, a harmonic angular swing [30, 4, 7, 22, 23], or a constant angular acceleration [26 etc.] is assumed and for these cases are the changes in the torque determined. Nevertheless, in the practice just the torque may be assumed to be known and the quantity searched for is the change in the angle, or in the slip describing the swing or other relative motion of the rotor.

The present paper discusses also a nonlinear problem on the whole, the asynchronous operation of turbo-generators. Though with an absolutely symmetrical rotor the slip would be — similar to that of the induction motors or generators — constant, in the turbo-generators realized up to now, even in those having a wholly cylindrical rotor, an asymmetry is caused by the field coil and this is the reason why a periodical change in the slip is arising.

The asynchronous operation is generally treated with in the books on the transient phenomena of synchronous machines, but only by assuming a *constant slip* [e. g. 3, 14, 23]. Even in the book discussing the asynchronous operation in a most detailed way [34] no treatment of the variable slip may be found.

So here may be also revealed the procedure outlined generally in the foregoing. Although it is evident that because of the asymmetry in the rotor the slip has to change, to avoid nonlinear differential equations, the slip is assumed to be constant and on the basis of the prescribed rotor motion taken in this way a priori, the torque is determined, and in the latter, as a consequence of the asymmetry, an average and pulsating component will arise, though in the reality the situation is the contrary: the torque is nearly constant, and the slip is changing. Here also the procedure so often applied in the engineering practice is adopted, not using a way of computation giving approximately true picture of the reality, but one supplying simple results. Author of the present paper followed also this way in his former works [6, 8, 9].

Studying the oscillograms relative to the asynchronous operation of turbo-generators, the question arose, if it is possible to elaborate a relatively simple method of engineering for determining first of all the variable slip, further the stator current and the reactive and apparent power.

The essence of the problem is, whether no simple method could be found for a simple solution of the nonlinear differential equation system describing the phenomena.

Naturally, the *step-by-step* method — similarly to the case of computing the dynamic, or transient stability — could be effective, but this is, though being an engineering method, quite a laborious and lengthy procedure for solving differential equations of second degree. Though adoption of the analog and digital computers could remove the difficulties involved in the step-by-step method — to-day this seems to be the most practicable way of solving the problems described by nonlinear differential equations — even if a great number of computers were available, the other *analytic methods* must be esteemed high as from theoretical as from practical point of view, especially if they give the solution in a closed form, as well as the simple *graphical constructions*, even if the results are less accurate.

Before giving an outline about the subjects to be dealt with, some remarks must be emphasized:

The differential equation of the problem analogous to that of the asynchronous operation of turbo-generators has been established decades ago [13] when studying the synchronization of synchronous machines. (To solve this problem, the differential analyzer method has been suggested.) Consequently, present treatise offers no new ideas when applying the above differential equation for the investigation of the variable slip.

On the other hand, no new ideas are suggested when showing the possibility to solve the above differential equation in a way differing from the step-by-step method either. In the second part of an engineering mathematical book [12] dealing with nonlinearities [17] published in 1942 the respective differential equation figures on page 210 in the following form:

$$\frac{d^2 \theta}{d \tau^2} + k(1 - b \cos 2 \theta) \frac{d \theta}{d \tau} + r \sin 2 \theta + \sin \theta = T$$

The left-side first term characterises the torque originating from the inertia (and the angular acceleration), the fourth term represents the synchronous torque, while the third one the reluctance torque. In the second term the slip is given by the differential quotient of the angle, its coefficient is not constant containing, however, the cosine function of the double angle too.

The book mentioned above [17] supplies after all the solution of the nonlinear differential equation by neglecting the term $\sin \theta$ (this corresponds just to the asynchronous operation of the de-excited machine). As a method of solution it adopts essentially the expansion in series and calculates the time functions of the angle, as well as the slip in form of an *infinite series*. Consequently this paper does not vindicate the claim of suggesting as first the calculation of the slip and the change in angle, respectively, in function of the time for asynchronous operation.

The solution mentioned above gives a clear picture about the advantages and disadvantages of the series expansion when solving the nonlinear differential equations. Although several methods of solution are known, the final result has generally a form of infinite series and a result in closed form (containing elementary functions of finite number), or a solution of higher order (containing at least tabulated functions) may be expected only exceptionally. Anyway, the solution obtained in form of an infinite series has undoubtedly the advantage of establishing the quantities searched for as an explicit function of the time. From an engineering viewpoint the series solution is especially advantageous if the series converges quickly, resulting a practically adequate accuracy when not considering, but some of the members. In any case, the terms of final number do not give, but an approximate value being perhaps near to the accurate one. It must be also considered, that already at the start, when having established the differential equation of the problem, some neglections were necessary. If the determination of the coefficients of the series is laborious (being the calculation of the coefficient next in turn always more troublesome, than the previous one), then engineering practice is satisfied with fewer members to the detriment of accuracy, or transforming the initial differential equation, looks for a faster converging solution. In searching for the solution methods of the nonlinear

differential equations, comprehension of the physical phenomena and preliminary estimation of the presumable characteristic of the solution (periodic, aperiodic, etc.) plays an important part. Opposite to the problems described by the linear differential equations, nonlinear cases demand always a certain individual treatment.

Consequently, the method followed in the present study cannot be expected to be of *general validity* in solving the nonlinear differential equations. The method exposed in this paper wishes to give new ideas *merely at the field of the asynchronous operation of turbo-generators*.

References [34, 35], but also home experiences [6, 7, 8, 9, 10] show the medium slip being very small: a magnitude of a thousandth (a tenth per cent). This renders reasonable the simplification of assuming an approximately constant torque and turbine power, respectively (also the solution exposed above considers a constant torque), hence the change in the speed of rotation remains within the insensitivity zone of the turbine regulator. In addition, not only the medium slip is small, but also the rates of change in the periodic slip are "slow", consequently, the first differential quotients may be neglected against the slip itself (and also against the current), that is, the term containing the inertia constant, as well as the additional torques being created as a consequence of the slip *change* may be left out of consideration.

Hence after all only the second member containing the slip and the third member characteristic of the reluctance torque remains on the left side of the aforesaid nonlinear differential equation. That is, the nonlinear differential equation is reduced with respect to the angular change to a first order one. Owing to the fact, however, that no time function figures at the right side, as the torque may be taken for constant, the differential equation belongs to a well-known class, that of the so-called *separable differential equations*. Nevertheless, separable differential equations may be solved by a simple integration, and at the very most the question arises, if there exists at all a primitive function and if the solution may be expressed by well-known functions. Author followed the method outlined already in some previous works [10, 19, 20] and succeeded in giving a closed form solution of the slip and the angular change for the most simple case. It is true, that opposite to the series expansion, the solution does not contain the time in an explicite form, nevertheless, in the mathematics and in the engineering practice the parametric establishment of the functions is just as much accepted, as the explicite form. Namely the solution mentioned give the time, as well as the slip in function of the angle, consequently it expresses the relation between slip and time by aid of the angle parameter. Although the solution — taking into account the above neglections — is only a first approximation, the result expressed in a *closed form* is advantageous as from theoretical, as from practical point of view.

Present serial treatise makes an important advance on the way commenced: it develops the procedure outlined to a method, and making use of the possibilities given by the method suggested, examines in details, on the general solutions of closed form, the influence of the different machine constants (damping factor, reluctance factor) upon the time function of the slip, the angle, the reactive power, etc.

The differential equation of second order mentioned many times in the foregoing, and also the simplified differential equation of first order originates from the essential simplification of the problem, namely — as we shall see — through substituting the admittance diagrams assumed to be circular, by their initial tangents, *i. e.* by the so-called primitive lines.

The method suggested permits to examine by analytic procedure other, substantially more complicated starting conditions too. Namely, the *approximation* of the admittance diagram of any (*i. e.* not of circular) form by a *generally situated straight line*, or *rendering it linear by sections*, or its *approximation by a parabola*. Finally — considering the rotor being of solid iron — the *graphical method* based on the procedure suggested will be elaborated taking in account the admittance diagrams of arbitrary form. Thereby the time function of the slip and the relative angle, as well as that of the stator current, the reactive and the apparent power may comparatively simply be determined.

The study finally compares the theoretical results with the oscillograms plotted in course of the experimental test of the asynchronous operation to state the justifiability of the neglects made and the efficiency of the method suggested.

Asynchronous operation of the synchronous machines is not autotelic, but permits, as it is generally recognized, to substitute the electrically damaged exciter for a reserve one during service, rendering thereby practically possible to increase the safety of the co-operative power system. Present paper does not discuss the possibilities, conditions and limitations of the asynchronous operation, as this field has been handled in details by the previously published studies and articles, as from the viewpoint of the turbo-generators, as from that of the network [34, 35, 6, 8, 9, 10, 11, 19, 20, 21].

1. Assumptions, conventions, fundamental equations

Before coming to the discussion of the subject: the methods for determining the variable slip in the steady-state asynchronous operation, a short summary will be given about the assumptions, and conventions applied in the theoretical study of the synchronous machines, and the fundamental relations will be indicated. The material summarized in this chapter presents merely an introduction for the further investigations.

1.1. Assumptions and conventions

In the fundamental works describing the transient behaviour of the synchronous machine [29, 30, 3, 14, 2, 23] the starting assumption is an idealized two-pole synchronous machine [27, 14, 1]. Present treatise accepts the usual simplifications, respectively agreements too. When using, however, the per unit system, we prefer to introduce the synchronous angular speed ω_0 in the expression, in order the equations should represent better the physical picture. Naturally, at any step $\omega_0 = 1$ may be substituted too, then simultaneously the time must be understood instead of seconds in radians.

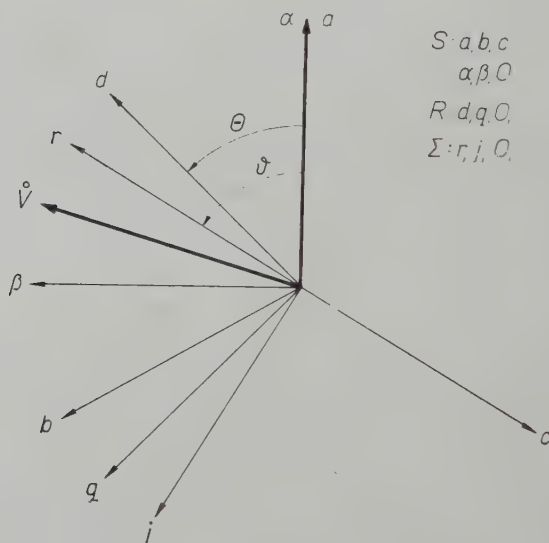


Fig. 1—1

By introducing the angular speed, respectively the angular frequency ω_0 , the form of voltage equations is valid for the quantities expressed both in the per unit system and in defined (volt, amper, ohm, etc.) one.

In addition to the generally accepted assumptions and conventions, treatise makes the following agreements:

All of the coils are assumed to be of right-side turn. Therefore the *positive direction* of the flux linkage, the voltage and the current are chosen to be the same [24].

The positive power hence corresponds to the power consumed, taken from the network. Similarly, the positive torque means a driving motor torque.

On the contrary, the negative power corresponds to the power supplied into the network and the negative torque represents a braking generator torque.

The sense of rotation of the rotor is counterclockwise. The magnetic axis of the stator phase windings is reached by the rotor in a sequence, a, b, c , hence the phase b leads phase a by 120 (electric) degrees, the phase c lags it by 120 (electric) degrees in the space. The positive direction of the quadrature axis q advances by 90 electric degrees the positive direction of the direct axis d (See Fig. 1—1).

Instead of the Laplace transform the study applies the more simple operational calculus (p is the differential operator $\frac{d}{dt}$), but the unit-functions are omitted.

The symbols applied here are of general use in literature. The complex vectors constant in time are marked by an upper line, *e. g.* \bar{v} (its conjugate is \hat{v}), while *e. g.* \dot{v} means a complex vector, variable in time (its conjugate is \dot{v}^*).

1.2. Co-ordinate transforms

In the study three kinds of co-ordinate systems occur (Fig. 1—1): *a)* the co-ordinate system S , fixed to the stator, being either a three-phase system, with axes a, b, c , placed at 120° from each other, or a two-phase system, with axes a, β being at right angle to each other; *b)* the co-ordinate system R , fixed to the rotor with the two-phase axes d, q ; *c)* the synchronously revolving co-ordinate system Σ with the real r and the imaginary j axis. The arbitrary vector \dot{v} ($v = u$ or ψ or i) may be written in the different co-ordinate systems by aid of the instantaneous values as follows:

$$\begin{aligned}\dot{v}_S &= \frac{2}{3}(v_a + \bar{a}v_b + \bar{a}^2v_c) = v_a + jv_\beta \\ \dot{v}_R &= v_d + jv_q \\ \dot{v}_\Sigma &= v_r + jv_j\end{aligned}\tag{1-1a}$$

where

$$\begin{aligned}\bar{a} &= -\frac{1}{2} + j\frac{\sqrt{3}}{2} = e^{j2\pi/3} \\ \bar{a}^2 &= -\frac{1}{2} - j\frac{\sqrt{3}}{2} = e^{-j2\pi/3}\end{aligned}\tag{1-1b}$$

as in balanced operation

$$v_0 = \frac{1}{3}(v_a + v_b + v_c)\tag{1-1c}$$

Let be (Fig. 1—1):

$$(a, d) \angle = \theta = \theta_0 + \omega t \quad (1-2a)$$

and

$$(a, r) \angle = \vartheta = \vartheta_0 + \omega_0 t \quad (1-2b)$$

so

$$(d, r) \angle = \vartheta - \theta = \vartheta_0 - \theta_0 + s \omega_0 t \quad (1-2c)$$

then the co-ordinate transforms are according to Fig. 1—1:

$$\begin{aligned} \dot{v}_S &= e^{j\theta} \dot{v}_R & \dot{v}_S &= e^{j\theta} \dot{v}_\Sigma \\ \dot{v}_R &= e^{-j\theta} \dot{v}_S & \dot{v}_R &= e^{j(\theta-\vartheta)} \dot{v}_\Sigma \\ \dot{v}_\Sigma &= e^{-j\vartheta} \dot{v}_S & \dot{v}_\Sigma &= e^{j(\vartheta-\theta)} \dot{v}_R \end{aligned} \quad (1-3)$$

1.3. Co-ordinate transform of the stator voltage equations

The three (or two) stator voltage equations may be established in the co-ordinate system S (a, b, c) in form of a single complex vector equation, as follows:

$$\dot{u}_S = p \dot{\psi}_S + r \dot{i}_S \quad (1-4)$$

As the mutual inductance between the stator and the rotor windings is a periodic function of the angle formed by the magnetic axes, to avoid differential equations with periodic coefficients, it is practicable to change over from co-ordinates S (a, b, c) to co-ordinates R (d, q).

Applying the co-ordinate transform equations, as well as Heavyside's shifting theorem, the stator voltage equations are from Eq. (1—4) in the co-ordinate system R (d, q):

$$\dot{u}_R = (p + j\omega) \dot{\psi}_R + r \dot{i}_R \quad (1-5a)$$

Separating the real and imaginary terms [29, 3, 1, 2, 5]:

$$\begin{aligned} u_d &= p \psi_d - \omega \psi_q + r i_d \\ u_q &= p \psi_q + \omega \psi_d + r i_q \end{aligned} \quad (1-5b)$$

Besides the induced (transformatory) voltage components also generated (rotary) voltage components arise, hence equations are now somewhat more

complicated, but have the great advantage, however, of being linear differential equations, with constant coefficients, if the rotor angular speed is constant [29, 3, 1, 2, 5].

Finally (similar to the foregoing) the voltage equation of the stator is in complex vector notation with respect to the synchronously revolving Σ (r, j) co-ordinate system

$$\dot{u}_{\Sigma} = (p + j\omega_0)\dot{\psi}_{\Sigma} + r i_{\Sigma} \quad (1-6)$$

14. Operational inductances

The relation between the flux-linkage components and the current components in the direct and quadrature axis, respectively, may be expressed as follows [3, 28, 29, 5]:

$$\begin{aligned} \omega_0 \psi_d &= \omega_0 l_d(p) i_d = x_d(p) i_d \\ \omega_0 \psi_q &= \omega_0 l_q(p) i_q = x_q(p) i_q \end{aligned} \quad (1-7)$$

where $l_d(p), l_q(p)$ and $x_d(p), x_q(p)$ are the so-called operational inductances, respectively, operational impedances.

Assuming on the rotor in addition to the field only a single direct-axis damping circuit and a single quadrature-axis damping circuit, the operational impedances may be written in the following form:

$$x_d(p) = x_d \frac{(pT_d'' + 1)(pT_d' + 1)}{(pT_{d0}'' + 1)(pT_{d0}' + 1)} \quad (1-8)$$

and

$$x_q(p) = x_q \frac{pT_q'' + 1}{pT_{q0}'' + 1}$$

Though the two amortisseur circuits do not replace the solid rotor, for the sake of simplicity, this is our starting assumption. Expanding in partial fractions, the operational impedances may be expressed as follows [23, 25, 38]:

$$\begin{aligned} x_d(p) &= x_d - (x_d - x_{d0}') \frac{pT_{d0}'}{pT_{d0}' + 1} - (x_{d0}' - x_d'') \frac{pT_{d0}''}{pT_{d0}'' + 1} \\ x_q(p) &= x_q - (x_q - x_q'') \frac{pT_{q0}''}{pT_{q0}'' + 1} \end{aligned} \quad (1-9)$$

while their reciprocals have the following form:

$$\begin{aligned} \frac{1}{x_d(p)} &= \frac{1}{x_d} + \left(\frac{1}{x'_d} - \frac{1}{x''_d} \right) \frac{pT'_d}{pT'_d + 1} + \left(\frac{1}{x''_d} - \frac{1}{x'_d} \right) \frac{pT''_d}{pT''_d + 1} \\ \frac{1}{x_q(p)} &= \frac{1}{x_q} + \left(\frac{1}{x'_q} - \frac{1}{x''_q} \right) \frac{pT'_q}{pT'_q + 1} \end{aligned} \quad (1-10)$$

1.5. Voltage equations of the stator

With regard to Eq. (1-7), the voltage equations (1-5b) may be written as follows:

$$\begin{aligned} u_d &= [p l_d(p) + r] i_d - \omega l_q(p) i_q \\ u_q &= \omega l_d(p) i_d + [p l_q(p) + r] i_q \end{aligned} \quad (1-11a)$$

respectively

$$\begin{aligned} u_d &= \left[\frac{p}{\omega_0} x_d(p) + r \right] i_d - \frac{\omega}{\omega_0} x_q(p) i_q \\ u_q &= \frac{\omega}{\omega_0} x_d(p) i_d + \left[\frac{p}{\omega_0} x_q(p) + r \right] i_q \end{aligned} \quad (1-11b)$$

finally, taking into account the relation $\omega = (1-s)\omega_0$:

$$\begin{aligned} u_d &= \left[\frac{p}{\omega_0} x_d(p) + r \right] i_d - (1-s) x_q(p) i_q \\ u_q &= (1-s) x_d(p) i_d + \left[\frac{p}{\omega_0} x_q(p) + r \right] i_q \end{aligned} \quad (1-11c)$$

In possession of the voltages, the currents may be determined:

$$\begin{aligned} i_d &= \frac{[p l_q(p) + r] u_d + \omega l_q(p) u_q}{[p l_d(p) + r] [p l_q(p) + r] + \omega^2 l_d(p) l_q(p)} \\ i_q &= \frac{-\omega l_d(p) u_d + [p l_d(p) + r] u_q}{[p l_d(p) + r] [p l_q(p) + r] + \omega^2 l_d(p) l_q(p)} \end{aligned} \quad (1-12)$$

Taking into consideration the expressions (1-8) of the operational inductances, the relations (1-12) get a quite complicated form. Neglecting, however, the stator resistance, considerable simplifications may be achieved:

$$\begin{aligned} i_d &= \frac{p u_d + \omega u_q}{(p^2 + \omega^2) l_d(p)} \\ i_q &= \frac{-\omega u_d + p u_q}{(p^2 + \omega^2) l_q(p)} \end{aligned} \quad (1-13)$$

1.6. Torque equations

The shaft of the synchronous generator is influenced by three torques: the mechanical driving torque of the turbine m_m , the electromagnetic (generally braking) torque m_e and the torque arising at angular acceleration or deceleration (resulting from the inertia) m_i . The resultant of the three torques is zero:

$$m_m + m_e + m_i = 0 \quad (1-14)$$

The electromagnetic torque may be written consecutively in the stator S , rotor R and synchronous Σ co-ordinate system — as it is known [e. g. 3] — in the following form:

$$\begin{aligned} m_e &= \psi_a \dot{i}_\beta - \psi_\beta \dot{i}_a \\ m_e &= \psi_d \dot{i}_q - \psi_q \dot{i}_d \\ m_e &= \psi_r \dot{i}_j - \psi_j \dot{i}_r \end{aligned} \quad (1-15)$$

The torque originating from the change in angular speed because of the inertia may be written as follows [e. g. 25, 23]:

$$m_i = -p T_m \frac{\omega}{\omega_0} = p T_m s \quad (1-16)$$

where T_m is the so-called mechanical time constant: it is twice the value of the kinetic energy stored in the revolving masses at synchronous speed related to the rated apparent power of the generator. If a constant torque, corresponding to the rated apparent power, affects the generator shaft, within this time T_m would the rotor accelerate from the rest up to the synchronous speed. It must be noted, that in the technical literature instead of T_m sometimes the symbol $2H$ may be found [23, 2, etc.], where H is the so-called inertia constant.

2. Fundamental equations of the asynchronous operation

In the following the fundamental relations of the asynchronous operation will be discussed. Though theoretically the consideration of the stator resistance would not involve difficulties, formula would get quite complicated and lengthy, rendering thereby heavier the perspicuity. As it was underlined in *clause 1.5*, neglectation of the stator resistance results in considerable simplifications. As when discussing the steady-state conditions, the stator resistance of small value does not influence, but slightly the results, the present study supplies the formula only for this more simple case.

2.1. Fundamental equations of the synchronous operation by assuming a constant slip

If the rotor runs with a constant slip s , the angle to be measured between the rotor and the revolving field changes linearly. Let us denote by δ the angle of the rotor direct axis as compared with the vector $\dot{\psi}$ of the synchronously revolving flux linkage at an arbitrary instant (Fig. 2—1); then evidently

$$\delta = \delta_0 - s \omega_0 t \quad (2-1)$$

as $-s \omega_0$ is the relative angular speed of the rotor with respect to the revolving field. It must be noted, that in an asynchronous motor operation the slip s

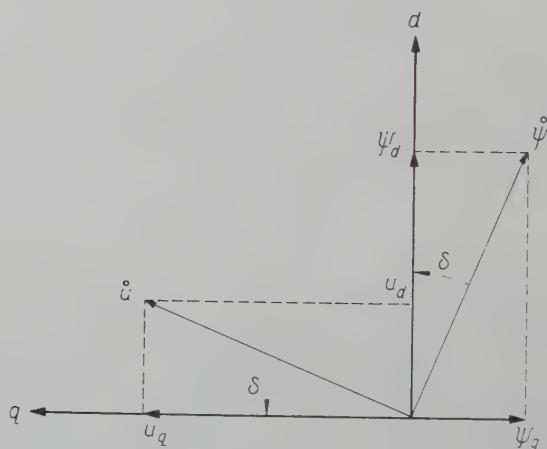


Fig. 2—1

is positive, consequently the angle δ is decreasing; on the contrary, in asynchronous generator operation, the slip s is negative, hence the angle δ is increasing.

In the co-ordinate system $R (d, q)$ of the rotor the vector of the flux linkage is

$$\dot{\psi}_R = \dot{\psi}_d + j \dot{\psi}_q = \dot{\psi} e^{-j\delta} \quad (2-2)$$

consequently the co-ordinates of the flux linkage are

$$\begin{aligned} \dot{\psi}_d &= \dot{\psi} \cos \delta \\ \dot{\psi}_q &= -\dot{\psi} \sin \delta \end{aligned} \quad (2-3)$$

The voltage equation in system R , according to (1—5a), by substituting $\omega = (1 - s) \omega_0$

$$\dot{u}_R = [p + j(1 - s) \omega_0] \dot{\psi}_R + r \dot{i}_R$$

which may be expressed on the basis of $r = 0$ and Eqs. (2—1). (2—2) for the steady state (by substituting the relation $p = -j s \omega_0$):

$$\dot{u}_R = [j s \omega_0 + j(1 - s) \omega_0] \dot{\psi}_R$$

Taking also the relation (2—2) into account

$$\dot{u}_R = u_d + j u_q = j \omega_0 \dot{\psi}_R = j \omega_0 \psi e^{-j\delta} = j u e^{-j\delta} \quad (2-4)$$

where

$$u = \omega_0 \psi \quad \text{respectively} \quad \psi = \frac{u}{\omega_0} \quad (2-5)$$

Accordingly, the vector of the terminal voltage leads by 90° the vector of the flux linkage and so the angle δ is at the same time the relative angle of the quadrature axis q with respect to the voltage vector \dot{u} (Fig. 2—1).

On the basis of Eq. (2—4), the co-ordinates of the voltage vector are in system R :

$$\begin{aligned} u_d &= \omega_0 \psi \sin \delta = u \sin \delta \\ u_q &= \omega_0 \psi \cos \delta = u \cos \delta \end{aligned} \quad (2-6)$$

As demonstrated in formula (2—1), the direct-axis and quadrature-axis components of the voltage and the flux linkage are harmonic functions of the slip frequency. Therefore the symbolic method, well-known from the alternating currents theory, may be applied for the arbitrary

$$v = u, \psi, i$$

variables

$$\begin{aligned} v_d &= \text{Re } \dot{V}_d \\ v_q &= \text{Re } \dot{V}_q \end{aligned} \quad (2-7)$$

So according to (2—6) *e. g.*:

$$\begin{aligned} \dot{U}_d &= j u e^{-j\delta} \\ \dot{U}_q &= u e^{-j\delta} \end{aligned} \quad (2-8)$$

and considering both Eq. (2—3) and Eq. (2—6)

$$\dot{\Psi}_d = \psi e^{-j\delta} = \frac{j u}{j \omega_0} e^{-j\delta} = \frac{1}{j \omega_0} \hat{U}_d \quad (2-9)$$

$$\dot{\Psi}_q = -j \psi e^{-j\delta} = -\frac{u}{j \omega_0} e^{-j\delta} = \frac{1}{j \omega_0} \hat{U}_q$$

On the basis of relations (1—7)

$$i_d = \frac{\psi_d}{l_d(p)} = \frac{\omega_0 \psi_d}{x_d(p)} \quad (2-10)$$

$$i_q = \frac{\psi_q}{l_q(p)} = \frac{\omega_0 \psi_q}{x_q(p)}$$

hence taking into account (2—9), and substituting besides $p = j s \omega_0$ for the steady state:

$$\dot{I}_d = \frac{\dot{\Psi}_d}{\bar{l}_d(j s \omega_0)} = \frac{\omega_0 \dot{\Psi}_d}{\bar{x}_d(j s \omega_0)} = \frac{\hat{U}_d}{j \bar{x}_d(j s \omega_0)} \quad (2-11)$$

$$\dot{I}_q = \frac{\dot{\Psi}_q}{\bar{l}_q(j s \omega_0)} = \frac{\omega_0 \dot{\Psi}_q}{\bar{x}_q(j s \omega_0)} = \frac{\hat{U}_q}{j \bar{x}_q(j s \omega_0)}$$

Introducing the symbols

$$\bar{y}_d = \bar{y}_d(j s \omega_0) = \frac{1}{j \bar{x}_d(j s \omega_0)} = \frac{1}{j \omega_0 \bar{l}_d(j s \omega_0)} \quad (2-12)$$

$$\bar{y}_q = \bar{y}_q(j s \omega_0) = \frac{1}{j \bar{x}_q(j s \omega_0)} = \frac{1}{j \omega_0 \bar{l}_q(j s \omega_0)}$$

(2—11) may be written after all in the following form:

$$\begin{aligned} \dot{I}_d &= \bar{y}_d \hat{U}_d = j u e^{-j\delta} \bar{y}_d \\ \dot{I}_q &= \bar{y}_q \hat{U}_q = u e^{-j\delta} \bar{y}_q \end{aligned} \quad (2-13)$$

With due regard to the current vector (2—7), expressed in the rotor coordinate system R

$$i_R = i_d + j i_q = \text{Re } \dot{I}_d + j \text{Re } \dot{I}_q = \frac{1}{2} (\dot{I}_d + \dot{I}_d^*) + j \frac{1}{2} (\dot{I}_q + \dot{I}_q^*) \quad (2-14)$$

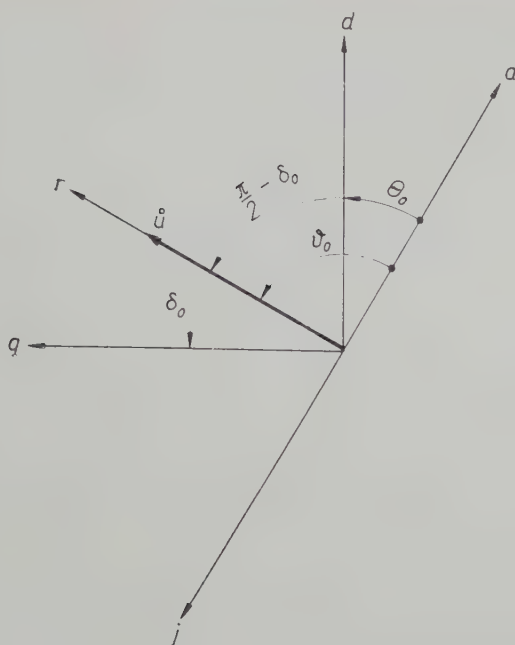


Fig. 2-2

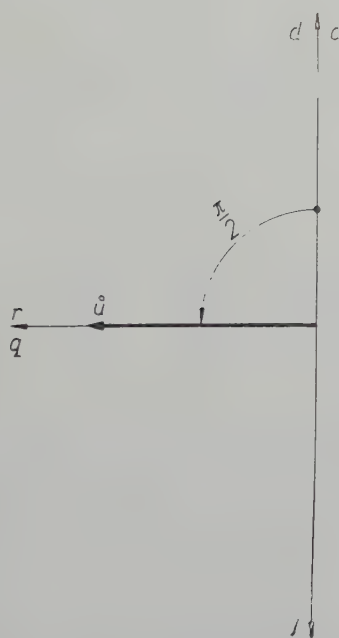


Fig. 2-3

which becomes, after substituting Eq. (2—13)

$$i_R = u \left[j \frac{\bar{y}_d + \bar{y}_q}{2} e^{-j\delta} - j \frac{\hat{y}_d - \hat{y}_q}{2} e^{j\delta} \right]$$

that is

$$i_R = j u e^{-j\delta} \left[\frac{\bar{y}_d + \bar{y}_q}{2} - \frac{\hat{y}_d - \hat{y}_q}{2} e^{j2\delta} \right] \quad (2-15)$$

and considering Eq. (2—4)

$$i_R = \hat{i}_R \left[\frac{\bar{y}_d + \bar{y}_q}{2} - \frac{\hat{y}_d - \hat{y}_q}{2} e^{j2\delta} \right] \quad (2-16)$$

Transforming into the synchronously revolving co-ordinate system Σ by aid of Eq. (1—3) using the relation

$$\hat{v}_\Sigma = e^{j(\theta-\delta)} \hat{v}_R$$

with the initial conditions according to

$$\vartheta_0 = \theta_0 + \frac{\pi}{2} - \delta_0$$

(Fig. 2—2), which may be realized most naturally by choosing

$$\delta_0 = 0, \quad \theta_0 = 0 \quad \text{and} \quad \vartheta_0 = \frac{\pi}{2}$$

(Fig. 2—3), that is, the initial situation of the rotor corresponds to the synchronous no-load position, we obtain after all for the voltage and the current vectors the following relations:

$$\hat{v}_\Sigma = u \quad (2-17)$$

$$i_\Sigma = u \left[\frac{1}{2} (\bar{y}_q + \bar{y}_d) + \frac{1}{2} (\hat{y}_q - \hat{y}_d) e^{j2\delta} \right] \quad (2-18)$$

In addition the complex vector of apparent power is:

$$\hat{S} = \hat{u} \hat{i} = u^2 \left[\frac{1}{2} (\bar{y}_q + \bar{y}_d) + \frac{1}{2} (\hat{y}_q - \hat{y}_d) e^{j2\delta} \right] \quad (2-19)$$

and finally the torque:

$$m = \frac{u^2}{\omega_0} \operatorname{Re} \left[\frac{1}{2} (\bar{y}_q + \bar{y}_d) + \frac{1}{2} (\dot{y}_q - \dot{y}_d) e^{j2\delta} \right] \quad (2-20)$$

The above four relations express the variation in the four main quantities, characterizing the turbo-generator working with constant slip in asynchronous operation. According to the first relation the terminal voltage is constant, consequently the voltage vector is in the synchronous co-ordinate system of constant magnitude and position. As per the second relation, the stator current fluctuates between a certain maximum and minimum value with double slip-frequency. (It must be noted that relation (2—18) gives of course only the envelope curve of the current alternating with the frequency of the mains.) The current vector describes in the synchronously revolving co-ordinate system a circle of excentric position. The apparent power changes similarly to the current. The torque fluctuates also between a certain minimum and maximum value.

It is worth to mention, that the time course of both the current and the apparent power, as well as that of the torque is characterized by the resultant admittance vector

$$\dot{y} = \frac{1}{2} (\bar{y}_q + \bar{y}_d) + \frac{1}{2} (\dot{y}_q - \dot{y}_d) e^{j2\delta}. \quad (2-21)$$

Let us examine in some more details the geometrical locus of the resultant admittance given by relation (2—21).

2.2. The resultant admittance diagram

The course of the current, power and torque mentioned in the previous clause 2.1 may be perspicuously represented by the admittance diagram (Fig. 2—4). The voltage vector u is directed towards the real axis of vertical position. For the negative slips characteristic of the asynchronous generator operation, both the admittance diagram $\bar{y}_d = \bar{y}_d(j s \omega_0)$ referring to the direct axis, and that $\bar{y}_q = \bar{y}_q(j s \omega_0)$ referring to the quadrature axis are situated below the negative imaginary axis. Choosing for an arbitrary s slip, but of the same magnitude the terminal points of the vectors \bar{y}_d respectively \bar{y}_q on the corresponding admittance diagrams, the arithmetical mean vector

$$\bar{y}_s = \frac{1}{2} (\bar{y}_q + \bar{y}_d) \quad (2-22)$$

initial (no-load) position mentioned above, then the radius vector displaces by an angle 2δ with respect to its initial position (consequently, while the rotor covers a full turn, the radius vector revolves two times in the counter-clockwise, positive sense of rotation). Hence at an arbitrary instant the resultant admittance vector is (Fig. 2—4):

$$\dot{y} = \bar{y}_S + \dot{y}_D e^{j2\delta} \quad (2-24)$$

Of course, in case of a constant slip, the instantaneous value of the current, the apparent power and also that of the torque may easily be read from the admittance vector diagram \dot{y} (Fig. 2—4) for any given time.

The maximum and minimum current (or apparent power) are characterized by points g_{\max} and g_{\min} respectively, where

$$y_{\max} = y_S + y_D, \quad y_{\min} = y_S - y_D.$$

On the other hand, the maximum and minimum torque are characterized by points g_{\max} and g_{\min} respectively, and the maximum and minimum active currents are given by the same two points.

Similarly, the maximum and minimum reactive currents are characterized by b_{\max} and b_{\min} respectively.

It may be noted here, that the admittance \dot{y} is expressed by the conductance g and susceptance b in the following form:

$$\dot{y} = g - jb \quad (2-25)$$

Similarly

$$\begin{aligned} \bar{y}_S &= g_S - jb_S \\ \bar{y}_D &= g_D - jb_D \end{aligned} \quad (2-26)$$

and

$$\begin{aligned} \bar{y}_d &= g_d - jb_d \\ \bar{y}_q &= g_q - jb_q \end{aligned} \quad (2-27)$$

consequently the relations (2—22) and (2—23) are not valid only for the admittances, but also for the conductances and susceptances separately too, hence

$$g_S = \frac{1}{2}(g_q + g_d) \quad b_S = \frac{1}{2}(b_q + b_d) \quad (2-22')$$

$$g_D = \frac{1}{2}(g_q - g_d) \quad b_D = \frac{1}{2}(b_q - b_d) \quad (2-23')$$

It must be mentioned that with the chosen symbols $b > 0$ in all cases, while in asynchronous motor operation $g > 0$ and in asynchronous generator operation $g < 0$ (similarly to the slip s).

By reason of notations (2—25)... (2—27), Eq.(2—24) gets the following form:

$$\dot{y} = g - jb = (g_S - jb_S) + (g_D + jb_D) e^{j2\delta} \quad (2-28)$$

that is

$$g = g_S + g_D \cos 2\delta - b_D \sin 2\delta \quad (2-29)$$

$$b = b_S - b_D \cos 2\delta - g_D \sin 2\delta \quad (2-30)$$

Summarizing, it may be stated that assuming a constant slip, by formula (2—28) the course of the total current and of the apparent power, by formula (2—29), however, the course of the active power and of the torque, while by formula (2—30) the course of the reactive current and of the reactive power may be obtained. Naturally, to get a current, the admittance or its components must be multiplied by voltage u , to get a power they have to be multiplied by the voltage square u^2 , and to get a torque, they must be multiplied by the expression u^2/ω_0 too. An especially simple relation may be obtained in the per unit system ($\omega_0 = 1$), if the voltage is just the rated one, i.e. it is of unit value: $u = 1$. In this case, namely, the numerical value of the admittance y indicates simultaneously the current and the apparent power too, the conductance g gives also the active current, the active power and the torque, while the susceptance b supplies also the reactive current and the reactive power.

2.3. The average and pulsating torque

The torque expressed in relation (2—20) may be resolved into two components: the first is the *average* torque

$$m_m = \frac{u^2}{\omega_0} \operatorname{Re} (\bar{y}_q + \bar{y}_d) \quad (2-31)$$

while the second the *pulsating* torque

$$m_p = \frac{u^2}{\omega_0} \operatorname{Re} \frac{1}{2} (\hat{y}_q - \hat{y}_d) e^{j2\delta} \quad (2-32)$$

As on the basis of Eqs. (2—12) and (1—10), after substituting $p = js\omega_0$:

$$\begin{aligned} \bar{y}_d = \bar{y}_d(js\omega_0) &= \frac{1}{jx_d} + \left(\frac{1}{jx'_d} - \frac{1}{jx_d} \right) \frac{js\omega_0 T'_d}{js\omega_0 T'_d + 1} + \\ &+ \left(\frac{1}{jx''_d} - \frac{1}{jx'_d} \right) \frac{js\omega_0 T''_d}{js\omega_0 T''_d + 1} \end{aligned} \quad (2-33)$$

and

$$\bar{y}_q = \bar{y}_q(js\omega_0) = \frac{1}{jx_q} + \left(\frac{1}{jx''_q} - \frac{1}{jx_q} \right) \frac{js\omega_0 T''_q}{js\omega_0 T''_q + 1}$$

therefore the expression of the average torque is

$$m_m = \frac{u^2}{2\omega_0} \left[\left(\frac{1}{x_d''} - \frac{1}{x_d'} \right) \frac{s\omega_0 T_d''}{1 + (s\omega_0 T_d'')^2} + \left(\frac{1}{x_d'} - \frac{1}{x_d} \right) \frac{s\omega_0 T_d'}{1 + (s\omega_0 T_d')^2} + \right. \\ \left. + \left(\frac{1}{x_q''} - \frac{1}{x_q'} \right) \frac{s\omega_0 T_q''}{1 + (s\omega_0 T_q'')^2} \right] \quad (2-34)$$

while that of the pulsating torque

$$m_p = \frac{u^2}{2\omega_0} \left\{ \left[\left(\frac{1}{x_q''} - \frac{1}{x_q'} \right) \frac{s\omega_0 T_q''}{1 + (s\omega_0 T_q'')^2} - \left(\frac{1}{x_d''} - \frac{1}{x_d'} \right) \frac{s\omega_0 T_d''}{1 + (s\omega_0 T_d'')^2} - \left(\frac{1}{x_d'} - \frac{1}{x_d} \right) \frac{s\omega_0 T_d'}{1 + (s\omega_0 T_d')^2} \right] \cos 2\delta - \right. \\ \left. - \left[\left(\frac{1}{x_q''} - \frac{1}{x_q'} \right) \frac{(s\omega_0 T_q'')^2}{1 + (s\omega_0 T_q'')^2} + \frac{1}{x_q} - \left(\frac{1}{x_d''} - \frac{1}{x_d'} \right) \frac{(s\omega_0 T_d'')^2}{1 + (s\omega_0 T_d'')^2} - \left(\frac{1}{x_d'} - \frac{1}{x_d} \right) \frac{s\omega_0 T_d'}{1 + (s\omega_0 T_d')^2} - \frac{1}{x_d} \right] \sin 2\delta \right\} \quad (2-35)$$

where according to Eq. (2-1) $\delta = \delta_0 - s\omega_0 t$.

In case of a constant slip, the time integral of the pulsating torque taken for a half slip period is of course zero.

Should the slip equal zero: $s = 0$, then the average torque component disappears, while the pulsating torque supplies the so-called reluctance torque:

$$[m_p]_{s=0} = m_r = \frac{u^2}{2\omega_0} \left(\frac{1}{x_q} - \frac{1}{x_d} \right) \sin 2\delta_0 \quad (2-36)$$

Should the slip but slightly differ from zero, so that the terms containing the square of the slip may be neglected, the whole torque may be expressed as follows:

$$m = \frac{u^2}{2\omega_0} \left\{ \left[\left(\frac{1}{x_d''} - \frac{1}{x_d'} \right) T_d'' + \left(\frac{1}{x_d'} - \frac{1}{x_d} \right) T_d' + \left(\frac{1}{x_q''} - \frac{1}{x_q} \right) T_q'' \right] - \right. \\ \left. - \left[\left(\frac{1}{x_d''} - \frac{1}{x_d'} \right) T_d'' + \left(\frac{1}{x_d'} - \frac{1}{x_d} \right) T_d' - \left(\frac{1}{x_q''} - \frac{1}{x_q} \right) T_q'' \right] \cos 2\delta \right\} s\omega_0 + \\ + \frac{u^2}{2\omega_0} \left(\frac{1}{x_d} - \frac{1}{x_q} \right) \sin 2\delta \quad (2-37)$$

It will be observed, that substituting instead of δ the value of θ and instead of $s\omega_0$ the differential quotient of the angle $d\theta/d\tau$, we get the second

and third term of the differential equation figuring in the introduction. This means, that in the above differential equation instead of the whole expression of the asynchronous torque, *its approximate expression valid only for small slips* is figuring.

The expression of the whole torque supplied by Eqs. (2—34) and (2—35) is quite complicated in spite of the many simplifications involved. The least admissible expedient seems to be the replacement of the solid iron by one direct-axis and one quadrature-axis damping coil, respectively, when according to Eq. (2—33) the quadrature-axis admittance diagram \tilde{y}_q describes a circle, while the direct-axis admittance diagram \tilde{y}_d is of double squirrel-cage character, which may be approximated by two circles [18]. The admittance diagrams \tilde{y}_q and \tilde{y}_d taking in consideration to a certain extent the effect of the solid iron mass, would have a much more complicated form [34]. This problem is not dealt with in the study, our task being the approximation of the real admittance diagrams by simple curves (straight lines, parabolic curves) in order to determine the variable slip. In the following the subject matter will be just the problem, what kind of approximations are sufficient and necessary to obtain the expression of the variable slip in a closed form. Consequently, formulae (2—33) may be regarded as a first approximation.

Though assumption of a constant slip leads to incorrect results — *e. g.* the torque varies between wide limits, or the angular displacement of the rotor is uniform — it means an important step in passing over to the case of the variable slip.

3. The method suggested for determining the variable slip

Present chapter expounds the method for determining the variable slip: after the starting assumptions the essence of the method suggested is discussed, and the further tasks are indicated.

3.1. Simplifying assumptions

Foreign [34, 35] and home measurements [6, 8, 10, 11] have shown alike, that during asynchronous operation the slip of turbo-generators is small, being of a thousandth (*i.e.* a tenth per cent) order of magnitude. Consequently, the turbine regulator having a zone of insensitivity of approximately $\pm 0,1$ per cent does not perceive at all, or only slightly the change in the speed.

The above circumstance inspires the first supposition of the method suggested: during asynchronous operation the turbine power remains approxi-

mately constant. As the speed differs but slightly from the synchronous one, and varies insignificantly, also the torque may be regarded as constant.

Starting from the measurement experiences — i.e. from the small and relatively slow change in the speed — also the second assumption seems to be right: no considerable error arises, when neglecting the effect of the inertia torques. *E.g.* with respect to the medium slip $s_m = 0.001$, assuming, exaggerating, a maximum rate of change in slip variation $(ds/dt)_{\max} = 0.001/\text{sec}$, the maximum value of the arising torque according to formula (1—16) with a too high mechanical time constant $T_m = 20$ sec, is as follows

$$(m_i)_{\max} = 20 \text{ sec} \cdot 0.001/\text{sec} = 0.02$$

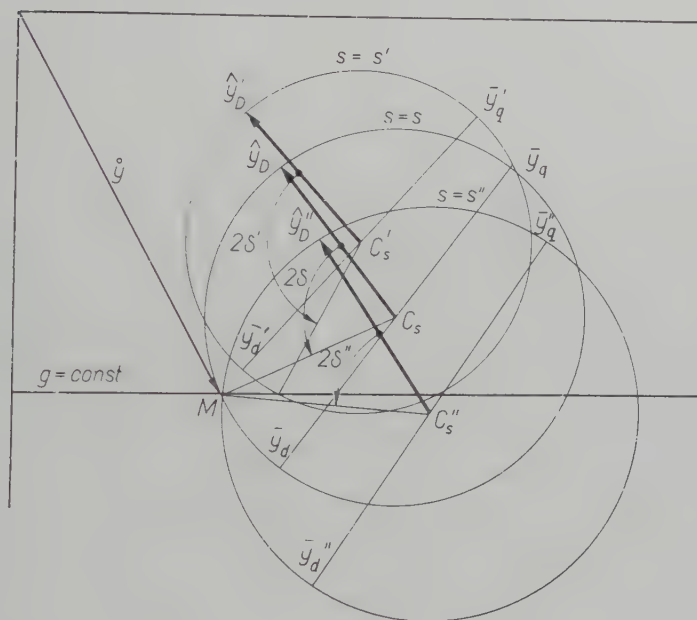


Fig. 3—1

As at the same time the driving torque of the turbine is at least

$$m_m = 0.4$$

neglection of the torque m_i introduces an error of at most 5 per cent.

Finally, the low value of the slip itself and of its variation in time renders the third assumption adopted plausible: in the calculations the static asynchronous torque-slip characteristic may be applied, neglecting therefore the effect of the change in the slip upon the torque curve.

These three assumptions are supported also by the periodic course of the slip, namely the error made at the angular acceleration is compensated by that arising at the angular deceleration.

Adoption of the three above simplifying assumptions permits us to apply further the resultant admittance diagram derived in *chapter 2*. Nevertheless, in the following, as the incorrect supposition of the slip being constant falls out, the starting assumption being the invariability of the active power (torque) and the active current, instead of a single admittance circle diagram C plotted for a certain constant slip (Fig. 2—4), now, on the one hand, a set of circle diagrams plotted for different slips must be traced, and, on the other hand, the terminal point of the resultant admittance vector has to move along the straight line $g = \text{const.}$, being parallel with the imaginary axis (Fig. 3—1).

3.2. The suggested method

In case of a variable slip and a constant torque the terminal points of the resultant admittance vectors are determined by the intersection of the straight line $g = \text{const.}$ and of the circles C_s plotted for different slips s (Fig. 3—1). On the plane of complex quantities, to each intersection belong at least three values: the conductance g taken as constant, the slip s belonging to the respective circle C_s , and the angle 2δ respectively δ to be determined from the initial \hat{y}_D and momentary $\hat{y}_D e^{j2\delta}$ position of the radius vector of circle C_s in question (Fig. 3—1). (Moreover the admittance \hat{y} and the susceptance b may be read.)

Owing to the fact that the equation of circles is given by formula (2—28), the relation between the values s and δ determined by the intersection of one of the circles and the straight line $g = \text{const.}$ is indicated by Eq. (2—29), having now the following form

$$g = g_s(s) + g_D(s) \cos 2\delta - b_D(s) \sin 2\delta \quad (3-1)$$

as, on the one hand, each circle C_s belonging to slip s has a different centre vector and radius vector, consequently $g_s(s)$, $g_D(s)$, $b_D(s)$ etc. are now functions of the slip s and, on the other hand, the resultant conductance g being constant, is independent of the slip.

As the relative angular speed is the differential quotient of the angle δ with respect to the time:

$$\frac{d\delta}{dt} = -s \omega_0 \quad (3-2)$$

the relation (3—1) is the differential equation of motion of the rotor. The dependent variable is the angle δ , the independent variable the time t . As

it may be seen, the relation (3—1) means a nonlinear differential equation given in implicate form.

The essence of the suggested method of solution is as follows :

Assume the slip s may be expressed from Eq. (3—1) as a function of the angle δ :

$$s = s(\delta) \quad (3-3)$$

Then Eq. (3—2) may be written as follows :

$$\frac{d\delta}{dt} = -s(\delta) \omega_0 \quad (3-4)$$

Should the angular value be $\delta = \delta_0$ at the initial time $t = 0$, then on the basis of Eq. (3—4):

$$-\int_{\delta_0}^{\delta} \frac{d\delta}{s(\delta)} = \int_0^t \omega_0 dt = \omega_0 t \quad (3-5)$$

Consequently, if the left-side integral exists, the time t is obtained as a function of angle δ :

$$t = t(\delta) \quad (3-6)$$

In conclusion, Eqs. (3—3) and (3—6) give indirectly the relation between the required dependent variable s and the independent variable t as functions of parameter δ . Accordingly, though in a parametric form, we succeeded in determining by $s(\delta)$ and $t(\delta)$ the desired relation

$$s = s(t) \quad (3-7)$$

Finally, with the aid of the inverse function of (3—6), the relation

$$\delta = \delta(t) \quad (3-8)$$

sought for is obtained too.

Substituting the relations (3—7) and (3—8) into expressions (2—28) and (2—29) respectively, which may be written similarly to (3—1) as follows

$$\dot{y} = (g_S(s) - j b_S(s)) + (g_D(s) + j b_D(s)) e^{j2\delta} \quad (3-9)$$

$$b = b_S(s) - b_D(s) \cos 2\delta - g_D(s) \sin 2\delta \quad (3-10)$$

the admittance vector

$$\dot{y} = \dot{y}(t) \quad (3-11)$$

as well as its absolute value

$$y = y(t) \quad (3-11')$$

and the susceptance

$$b = b(t) \quad (3-12)$$

are produced after all as functions of time. Consequently, the course of the apparent power and the stator current, as well as of the reactive power and reactive current may be obtained in function of the time.

3.3. Versions of the method suggested

Usefulness of the method exposed in *clause 3.2* depends substantially upon two circumstances: whether we succeed in expressing the relation (3—2) in an explicit form from Eq. (3—1) and whether the integral figuring at the left-side of Eq. (3—5) can be calculated, namely in a possibly closed form.

Consequently, study regards as its task in the following just to look for simple approximations assuring success in both steps and at the same time not leading to unacceptable results.

Application of the form of the admittances expressed in Eq. (2—33) must evidently be avoided, as it would create an equation of too high degree in the relation (3—1). An even smaller hope might be for adopting the more complicated admittance expressions considering more exactly the effect of the solid iron. (Naturally by the use of digital computers, the two possibilities now refused may be of question too.)

On the contrary, approximating the direct-axis and quadrature-axis admittance diagrams by straight lines, or by quadratic parabolas, the success of the first step is assured, as for the slip s only an equation of first — or second degree must be solved. The integrability remains, however, an undecided problem.

On the other hand, if the direct-axis and quadrature-axis admittance diagrams were as a result of other measurements available — plotting of the admittance diagram on the basis of measurements is, but lately dealt with [e.g. 31] — then the intersection assembly of the set of circles C_s with the straight line $g = \text{const}$, i.e. the values s and δ belonging to each other may be established, and then the integral figuring on the left-side of equation (3—5) may be determined by planimetry, by graphic, or numeric integration. The other steps included in *clause 3.2* can be realized without difficulty.

In this way the field of the further examinations may be outlined as follows:

a) Approximation by straight lines of the direct-axis and quadrature-axis admittance diagrams (linear approximation).

- b) Approximation of the above admittance diagrams by parabolas (quadratic approximation).
 c) Graphical construction.

Summary

Present paper — being the first part of a series consisting of several articles — makes a review of the methods applied till now for the theoreticale xamination of the turbo-generators in asynchronous operation and suggests a relatively simple method for the solution of the essentially nonlinear problem. The exposition and application of the method suggested will be discussed in the articles to be published later. For the preparation of this task, the fundamental relations serving as the starting point may be found here.

References

1. ADKINS, B.: Transient Theory of Synchronous Generators Connected to Power Systems. Proceedings of I.E.E. 1951. p. 510.
2. ADKINS, B.: The General Theory of Electrical Machines. Chapman and Hall. London, 1957.
3. CONCORDIA, C.: Synchronous Machines. Theory and Performance. John Wiley — Chapman and Hall. New York—London, 1951.
4. CRARY, S. B.: Two-Reaction Theory of Synchronous Machines. Electr. Eng. Trans. Jan. 1937. p. 27.
5. CSÁKI, F.: Influence of Series Capacitors on the Operation of Synchronous Machines. Acta Technica, 1955. XII. 1—2. p. 49.
6. CSÁKI, F.: Turbogenerátorok aszinkron üzeme. I. VILLENKI Közlemények, 1955. № 92.
7. CSÁKI, F.: Influence of Series Capacitors on the Operation of Synchronous Machines. Synchronizing and Damping Torques. Acta Technica, 1956. XV. p. 456.
8. CSÁKI, F.: 44 000 kVA-es turbogenerátor aszinkron üzeme. Elektrotechnika, 1956. № 8.
9. Чаки, Ф.: Исследование некоторых режимов работы синхронных генераторов в Венгрии. Электричество, 1957. № 12. ст. 44.
10. CSÁKI, F.: Turbogenerátorok aszinkron üzeme II. VILLENKI Közlemények, 1957. № 179.
11. CSÁKI, F.: Szinkron generátorok üzemének néhány kérdése. Elektrotechnika, 1958. № 4—6. p. 204.
12. DOHERTY, R. E.—KELLER, E. G.: Mathematics of Modern Engineering. Volume I. John Wiley — Chapman and Hall. New York—London, 1942.
13. EDGERTON, H. E.—FOURMARIER, P.: The Pulling into Step of a Salient Pole Synchronous Motor. Trans. A.I.E.E. 50 (June 1931).
14. Горев, А. А.: Переходные процессы синхронной машины. Госэнергоиздат, 1950.
15. Янко-Триницкий, А. А.: Электромеханические переходные процессы в синхронных машинах. Электричество, 1957. № 8. ст. 16.
16. Назовский, Е. Я.: Некоторые вопросы переходных процессов в машинах переменного тока. Госэнергоиздат, 1953.
17. KELLER, E. G.: Mathematics of Modern Engineering. Volume II. John Wiley — Chapman and Hall. New York—London, 1945.
18. Kovács, K. P.—RÁCZ, I.: Váltakozóáramú gépek tranziens folyamatai. Akadémiai Könyvkiadó. Budapest, 1954.
19. Kovács, K. P.—CsÁKI, F.: Asynchronbetrieb von Turbogeneratoren. Technische Rundschau, 1957. № 44. p. 3.
20. Kovács, K. P.—CsÁKI, F.: Marche asynchrone des turbo-alternateurs. CIGRÉ Rapport, № 115. Paris, 1958.
21. Kovács, K. P.—CsÁKI, F.: Asynchronous Running of Turbo-Generators. Periodica Polytechnica, Electrical Engineering, 1959. Vol. III. № 1. p. 1.

22. KRON, G.: A Short Course in Tensor Analysis For Electrical Engineers. John Wiley. — Chapman and Hall. New York—London, 1942.
23. LAIBLE, TH.: Die Theorie der Synchronmaschine im nichtstationären Betrieb. Springer-Verlag. Berlin /Göttingen/ Heidelberg, 1952.
24. LISKA, J.: Villamosgépek vektorábrái. Mérnöki Továbbképző Intézet, Budapest, 1944.
25. МАМИКОНЯНЦ, Л. Г.: Токи и моменты вращения, возникающие в синхронной машине при включении ее способом самосинхронизации. Труды ЦНИЭЛ IV. Госэнергоиздат, 1956.
26. МАМИКОНЯНЦ, Л. Г.: Токи и моменты асинхронных и синхронных машин при изменении скорости их вращения. Электричество, 1958. № 8. ст. 54.
27. PARK, R. H.: Definition of an Ideal Synchronous Machine and Formulae for the Armature Flux Linkage. General Electric Review. 31 (1928) p. 332.
28. PARK, R. H. — ROBERTSON, B. L.: The Reactances of Synchronous Machines. Trans. Amer. Inst. Electr. Engrs. 47 (1928) p. 514.
29. PARK, R. H.: Two-Reaction Theory of Synchronous Machines. Part I. Trans. Amer. Inst. Electr. Engrs. 48 (1929) p. 716.
30. PARK, R. H.: Two-Reactions Theory of Synchronous Machines. Part II. Trans. Amer. Inst. Electr. Engrs. 52. (1932) p. 352.
31. SEN, S. K. — ADKINS, B.: The Application of the Frequency-Response Method to Electrical Machines. Proceedings of the I.E.E. Part C. May 1956. Monograph No 178. S.
32. SHOULTS, D. R. — CRARY, S. B. — LAUDER, A. H.: Pull in Characteristics of Synchronous Motors. Electr. Eng. 54. (December 1935.)
33. STOKER, J. J.: Nonlinear Vibrations in Mechanical and Electrical Systems. New York, 1950.
34. Сыромятников, И. А.: Режимы работы синхронных генераторов. Госэнергоиздат, 1952.
35. Следнев, М. С.: Испытания турбогенераторов при работе в асинхронном режиме. Электрические станции, 1954. № 1. ст. 23.
36. Толмач, И. М.: Переходные процессы в синхронных электродвигателях при ударной нагрузке электричество, 1959. № 4. ст. 72.
37. Трещев, И. И.: Исследование машин переменного тока при переменной скорости вращения. Электричество, 1957. № 2. ст. 49.
38. WARING, M. L. — CRARY, S. B.: Operational Impedances of Synchronous Machines. General Electric Review, 35. (1932) p. 578.

Prof. F. Csáki, Budapest, XI., Egry József u. 18.

POWER PLANTS

Complete steam power plants, including heating power plants and back-pressure power plants for industry purposes more-over every element of power plants (boilers, coal handling equipment, water softener, steam turbine units, switching equipments, transformers).

Complete hydraulic plants (water turbine-alternator units, switching equipments, including penstocks and sluices, etc.). Steam turbine units up to 50 MW with condensing, back-pressure and bleeding type turbines. Water turbine-alternator units, Pelton, Francis and Kaplan turbines.

Transformer stations, switching equipments (switching stations).

Prof. Heller's Air-Cooled Condensers. / Transmission lines up to 132 kV.



PANORAMIC VIEW OF IKIZDERE POWER PLANT

panorama of the Ikizdere (Turkey) Hydro-Electric power Plant during erection. The complete Hydro-Mechanical and Electrical installation of the power plant including 3 Francis turbines of 7650 HP output, 3 alternators of 6500 kVA output and 6300 Voltage, a 6,3/66 kV step-up and four step-down transformer stations as well as a Transmission Line of 66 kV and 105 km length was delivered by KOMPLEX Hungarian Trading Company for Factory equipments. The plant will be completed by the end of 1960.



HUNGARIAN TRADING COMPANY FOR FACTORY EQUIPMENTS
BUDAPEST 36, P. O. B. 51.

Cable: "KOMPLEX BUDAPEST"

Short-wave and Medium-
wave Broadcasting
Transmitters

Mobile and Portable
Transmitterreceivers

Transmission Measuring
Instruments

High Frequency
Generators

CB and LB Telephone
Apparatus

CB and LB Switchboards

Automatic Telephone
Exchanges

Repeater Station
Equipments

Multichannel Carrier
Equipments

Microwave Multiplex
Equipments



BUDAVOX

Budapest Telecommunication Company

Budapest VII. Tanács krt. 3 a Telephone: 426 549

Letters: Budapest 62 P. O. B. 267

Cables: Budavox Budapest Telex: 672

A Budapesti Műszaki Egyetem Periodica Polytechnica címen idegen nyelvű tudományos folyóiratot indított. A folyóirat három sorozatban — vegyészeti, villamossági, valamint gépész- és általános mérnöki sorozatban — jelenik meg, évente négyszer, sorozatonként egy-egy kötetben. Az egyes kötetek terjedelme 14—18 ív.

A Periodica Polytechnicában megjelenő tanulmányok szerzői az Egyetem tanári karából és tudományos dolgozóiból kerülnek ki. Főszerkesztő Dr. Csűrös Zoltán egyetemi tanár, akadémikus.

A folyóirat előfizetési ára sorozatonként és kötetenként 60,— Ft. Megrendelhető az Akadémiai Kiadónál (Budapest 62, Postafiók 440. NB. egyszámlaszám: 05-915-111-46), a külföld számára pedig a Kultúra Könyv és Hírlap Külkereskedelmi Vállalatnál (Bp. 62, Postafiók 149, NB. egyszámlaszám: 43-790-057-181), illetve a vállalat külföldi képviselőinél és bizományosainál.

INDEX

FRIGYES, A.: About the Balancing of Half-Wave Push-Pull Magnetic Amplifiers	55
CSEERNÁTONY-HOFFER, A.: Stoßfestigkeitsprobleme der Trenn- schalter in Mittelspannungs-Innenraumanlagen	79
AMBRÓZY, A.: Statistical Quality Control Using an Analogue Computer	97
CsÁKI, F.: Theoretical Methods Concerned with the Asyn- chronous Operation of Turbo-Generators	117